PNL-2265-2
UC-70

Quarterly Progress Report Research and Development Activities Waste Fixation Program April Through June 1977

J. L. McElroy

July 1978

Prepared for the U.S. Department of Energy
under Contract No. EY-76-C-06-1830

Pacific Northwest Laboratory
Operated for the U.S. Department of Energy
by

Battelle
Memorial Institute

PNL-2265-2

NOTICE

PACIFIC NORTHWEST LABORATORY
operated by
BATTELLE
for the
UNITED STATES DEPARTMENT OF ENERGY
Under Contract EY-76-C-06-1830

Printed in the United States of America
Available from
National Technical Information Service
United States Department of Commerce
5285 Port Royal Road
Springfield, Virginia 22151

Price: Printed Copy $____*; Microfiche $3.00

*Pages	NTIS Selling Price
001-025	$4.50
026-050	$5.00
051-075	$5.50
076-100	$6.00
101-125	$6.50
126-150	$7.00
151-175	$7.75
176-200	$8.50
201-225	$8.75
226-250	$9.00
251-275	$10.00
276-300	$10.25

DISCLAIMER

PNL-2265-2
UC-70

QUARTERLY PROGRESS REPORT
RESEARCH AND DEVELOPMENT ACTIVITIES
WASTE FIXATION PROGRAM
APRIL THROUGH JUNE 1977

J. L. McElroy

July 1978

Prepared for
the U.S. Department of Energy
under Contract No. EY-76-C-06-1830

Pacific Northwest Laboratory
Richland, Washington 99352

PREVIOUS REPORTS

Previous reports in this series were BNWL-1699, 1741, 1761, 1788, 1809, 1826, 1841, 1871, 1893, 1908, 1932, 1949, 1994, 2070, 2242, 2243, 2264, and 2265-1.

SUMMARY

Through the Waste Fixation Program, the Pacific Northwest Laboratory is directing research on the solidification of high-level radioactive waste. A major goal of this program is to develop reliable waste glass compositions and processes for their manufacture. This progress report describes the research and development activities of the past quarter:

- A 36-inch diameter spray calciner coupled to a 210 KWA electrical resistance in-can melter, capable of accepting canisters 24 in. in diameter by approximately 9 ft long, was placed in operation. In initial tests, a waste feed rate of 210 liters/hour and a melting rate of 60 kg glass/hour were demonstrated.
- Leach rates of multiple samples from five nonradioactive simulated waste glass canisters (runs ICM-16, -18, -20, -21, and -34) show good uniformity for the glass in the 8 to 16 in. diameter canisters.
- X-ray diffraction measurements on supercalcine containing 3 wt% ^{244}Cm show that the radiation is causing the apatite phase to become amorphous. Fluorite and tetragonal phases are unaffected after three months.
- Self-decontamination of waste canisters (WSEP canisters SS-7 and PG-2) in a mini-wet basin was demonstrated. In the first 150 days, 86% of the initial smearable contamination was removed.
- Simulated waste glass marbles, encapsulated in an Al-12Si matrix were examined microscopically after 10-day heat treatments at 300 and 500°C. No reaction between the glass and metal matrix was observed.

CONTENTS

LIST OF FIGURES

LIST OF TABLES

QUARTERLY PROGRESS REPORT
RESEARCH AND DEVELOPMENT ACTIVITIES
WASTE FIXATION PROGRAM
APRIL THROUGH JUNE 1977

INTRODUCTION

The high-level Waste Fixation Program (WFP) is directed by the Pacific Northwest Laboratory (PNL), operated by Battelle Memorial Institute for the Department of Energy (DOE). Under this program, PNL is conducting research to convert high-level radioactive waste to stable nondispersible forms, such as silicate glasses. The WFP is designed to be a means through which users of the technology and the government can cooperate to effectively handle nuclear waste. Objectives of the comprehensive program include the development and characterization of glass formulations; equipment and process development; and design, construction, and demonstration of full-scale process equipment. The following sections describe research and development activities in radioactive waste fixation for the past quarterly reporting period.

SECTION 1 - WASTE FIXATION PROCESS DEVELOPMENT

The purpose of this task is to develop processes and equipment for converting liquid high-level radioactive waste to a stable, relativley nondispersible form for storage and, ultimately, disposal. This objective is generally being accomplished by development of a two-step approach (calcination and concentration) followed by melting to form a silicate glass.

FULL-SCALE SPRAY CALCINER/IN-CAN MELTER (NON-RADIOACTIVE) - A. A. Garrett, H. T. Blair, L. S. Romero, M. T. Killinger and T. L. Congdon

The objective of the non-radioactive Full-Scale Spray Calciner/In-Can Melter System (FSSC/ICM) is to demonstrate: large-scale throughputs (>200 liters/hour); long-term operation (30 days continuous); and key remote features for a full-scale, coupled system.

Design work began on the FSSC/ICM system in mid-1975; designs were finalized and procurement began in early 1976. Construction started in late 1976 and operation began in April 1977. Since April, a waste feed rate of 210 liters/hour and a melting rate of 60 kg glass/hr have been demonstrated. Higher throughputs are anticipated later this year.

The new system is shown in Figures 1, 2, and 3. Liquid waste is sprayed into an externally heated calcining chamber where it is dried and mixed with glass powder. Entrained particles are removed from the off gas by sintered metal filters. The calcine/glass powder mixture flows into a second furnace where it melts. The melting crucible also serves as a portable storage container for the vitrified waste.

The full-scale spray calcine and in-can melter physical parameters are listed in Tables 1 and 2. Currently, PNL uses a pressurized feed system involving a feed tank, pump and agitator. A brief description of the feed system is given in Table 3.

Future plans include 3-, 10-, and 30-day continuous runs to determine the maximum capacity of the system. Later the full-scale spray calciner will be coupled to a full-scale ceramic melter.

IN-CAN MELTING - H. T. Blair and W. J. Mikols

The purpose of this study is to further develop and to demonstrate on a full scale the vitrification of calcined high-level nuclear waste, using the storage can as the melting crucible.

A can of simulated, vitrified, high-level nuclear waste containing eight radial heat transfer fins made from E-Brite 26-1 alloy was sectioned for evaluation. The alloy has a thermal expansion coefficient very close to that of glass. Fracturing of the glass around the fins was significantly reduced when compared to that occurring around fins made with 304L stainless steel. Very little reaction between metal and melt occurred. The fin surfaces were smooth and the corners were sharp. Because of these results, heat transfer fins made from the E-Brite 26-1 alloy were used in the first two full-scale in-can melter cans.

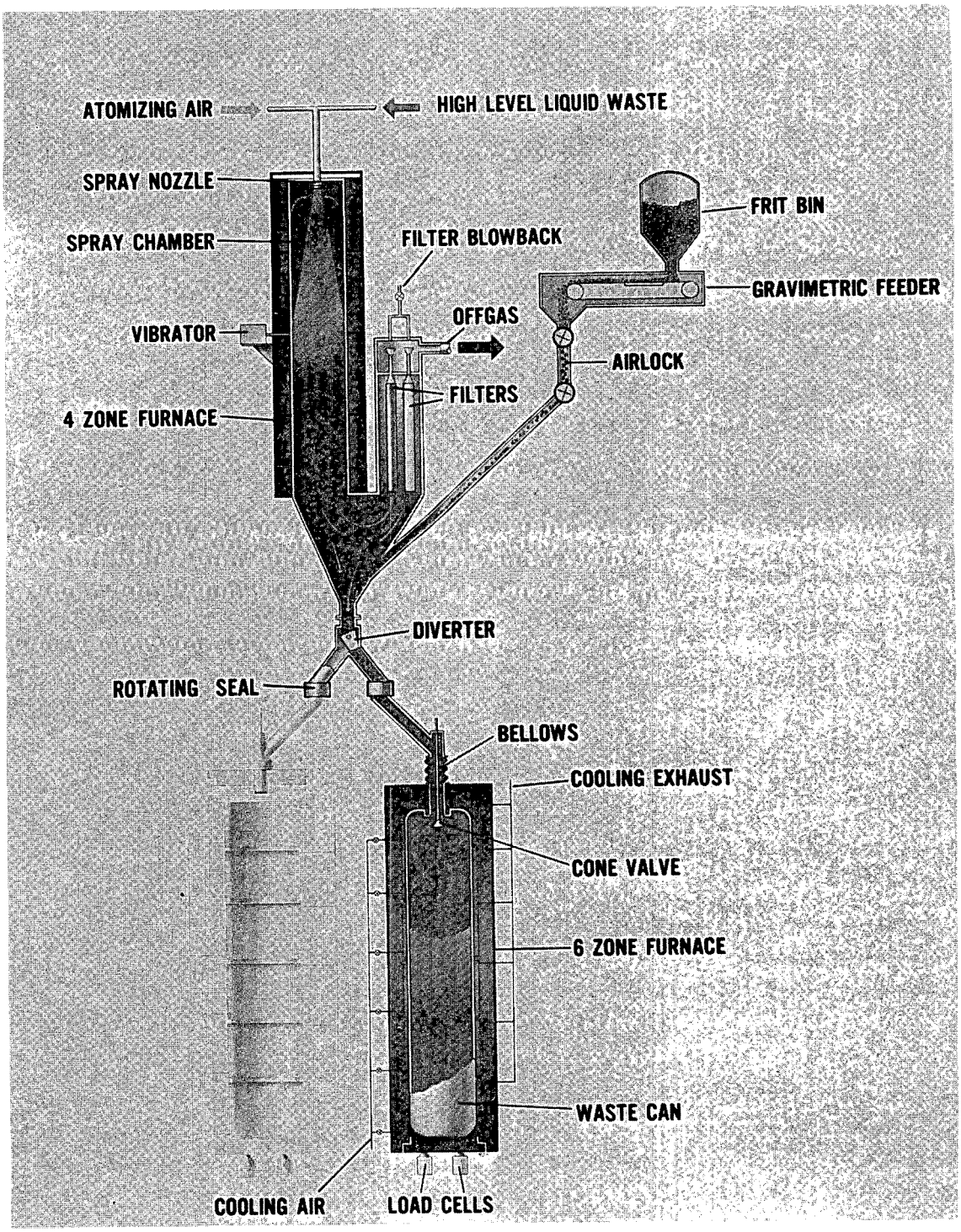

FIGURE 1. Spray Calciner/In-Can Melter Process

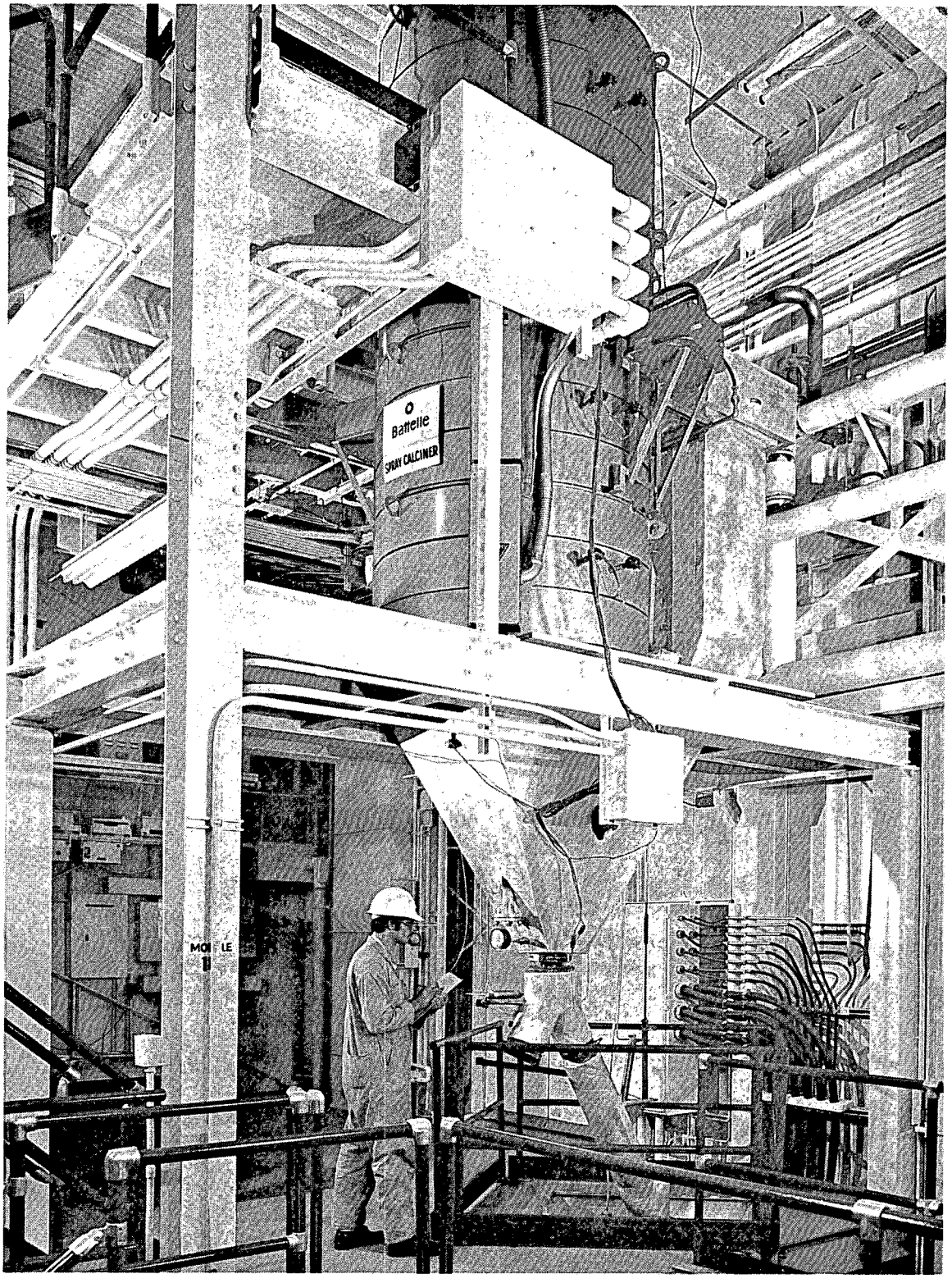

FIGURE 2. Full Scale Spray Calciner

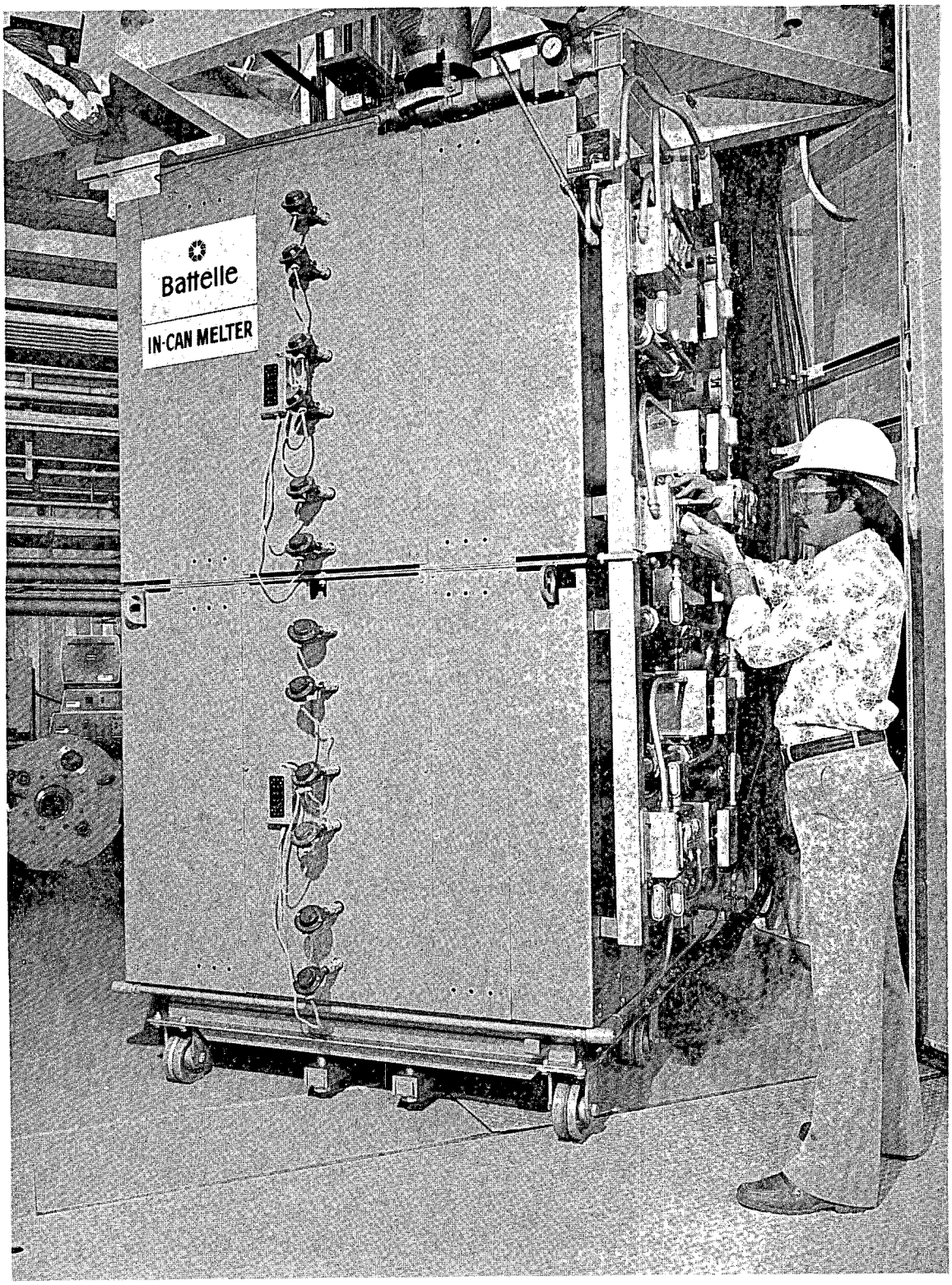

FIGURE 3. Full Scale In-Can Melter

TABLE 1. Full-Scale Spray Calciner

Spray Chamber

Length	10 ft, 6 in.
Diameter	36 in.

Cone

Vertical Length	52 in.
Slope	60°

Filter Chamber

Number of Filters	85
51	10μ Pore Size
34	65μ Pore Size
Total Surface Area	168 ft^2
Filter Size	36 in. x 2.75 in.

Spray Nozzle

Type: Internal Mixing
Orifice: 1/4 in., Ceramic

Vibrator

Type: Pneumatic, Side Mounted
Manufacturer: Cleveland Vibrator Company

Furnace

Type: Electrical Resistance
Power: 320 KVA
4 Zones Independently Controlled
Operating Temperature: 800°C
Size: 5 ft, 10 in.

TABLE 2. Full-Scale In-Can Melter

ICM Furnace

Type: Electrical Resistance
Power: 210 KVA
6 Zones Independently Controlled
Operating Temperature: 1050°C
Cooling: 50 kW
Size: 55 in. square x 9 ft, 6 in. long
Accepts 12 in. to 24 in. diameter Canisters

Calciner/Melter Connection

Continuous/Batch Transition: Two-way Diverter
Duct Size: 4 in.
Minimum Slope: 60°
Frit Addition Rate: Proportional to Calciner Feed Rate

Canisters

304L Stainless Steel Pipe
Schedule 40 and 80
Fusion Welded

TABLE 3. Feed System

Feed Tank

Capacity: 200 Gal (750 ℓ)
Size: 40 in. Diameter x 42 in.

Feed Pump

Recessed Impeller
Cantilever Type
Maximum Head 100 ft

Agitation

Propeller Type Agitator with 9 in. Prop
Bypass Feed Jet Mixer

Feed Control

Flow Meter and Control Valve

Frit Feed

Weight Belt Type Feeder
Air Lock Valve
Frit enters Lower Cone

During the past quarter, a non-contact thermowell device was developed to monitor ICM canister surface temperatures during process operation. The thermowell concept involves the monitoring of radiant heat from a canister's surface to evaluate its temperature. Experimental data show that such a device provides excellent temperature data (within 2°C) for steady state wall temperatures above 800°C. Transient canister surface temperatures can be monitored to within 5°C.

A high-sodium defense-waste sludge composition has been identified for preliminary in-can melting studies. Fabrication of the first two Inconel canisters for these studies is underway. Melting experiments in these canisters will generate some of the first ICM process data for this canister material. Initial defense-waste ICM studies will be aimed at evaluating this process for handling defense waste compositions.

FLUIDIZED-BED CALCINATION - J. C. Hartl, F. E. Haun and W. J. Bjorklund

Fluidized-bed calcination studies provide data for process and equipment development for the conversion of simulated high-level waste to a solidified form. The calcine product can then be fed directly or indirectly to a melting system for vitrification.

Several changes have been made in the operation of the Fluidized Bed Calciner (FBC). A cyclone has been added, allowing the continuous removal of calcine and bed material through an off-gas line placed immediately above the bed region. This operating technique has three major advantages:

- A disengaging chamber is not required on the calciner, considerably reducing equipment size.
- The bed overflow valve has been removed, reducing the complexity of the equipment and eliminating the potential for solids to plug the overflow line while the valve is closed.
- The product has a more uniform composition.

Another change in the operating procedure has been the addition of glass-forming chemicals to the feed. With the glass-forming compounds in the feed solution, a frit feeding mechanism is not required; this reduces equipment complexity and size. The calcine and glass-formers are more evenly mixed and their relative concentrations can be better controlled than by using a solids feed for frit addition.

A proposed operating change is the use of a sand bed filter as a replacement for, or prior to, sintered metal filters. Off gas from the cyclone would be passed through the silica sand, which is added as the inert bed material. Filter material would be continuously replaced, eliminating the possibility of filter binding. Material trapped in the filter would be automatically returned to the calciner, eliminating the need for equipment to handle and transport filter fines. A fluidized bed calciner incorporating these changes is shown in Figure 4. Additional work in this area includes:

- preparing for runs with defense-type waste, and
- conceptual design of a 500 ℓ/hr and a 1000 ℓ/hr FBC for the Savannah River Laboratory.

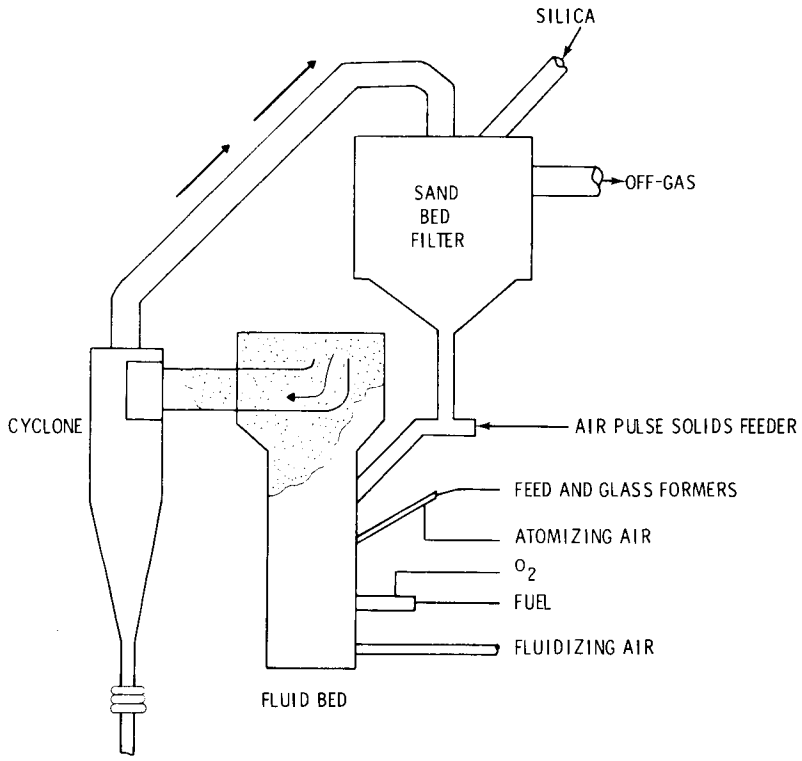

FIGURE 4. Revised Fluidized Bed Calciner

CONTINUOUS MELTING TASK - C. C. Chapman

The objective of this task is to develop the technology required to design, license, construct, and operate two radioactive waste vitrification processes. The two processes are: 1) a calciner-coupled ceramic melter, and 2) a direct liquid-fed ceramic melter.

The direct liquid-fed melter (DLF) has been at operating temperature since startup in early February. Short tests have shown that the unit is capable of processing at a rate of 85 ℓ/hr. The tilt-pour-drain technique has been successfully demonstrated in many tests.

The engineering-scale ceramic melter was disassembled and inspected after 23 months of operation at molten glass temperatures. The melter has demonstrated the successful feeding of calcined, simulated nuclear wastes and liquid simulated nuclear waste. The inspection revealed that the refractory brick and the metal electrodes were in very good condition. The melter probably could have been satisfactorily operated for an additional year.

In addition, we have designed a plant-scale ceramic melter which will be coupled to the full-scale spray calciner. Construction of the unit will begin soon.

SECTION 2 - WASTE FORM CHARACTERIZATION

The purpose of waste form characterization is to measure the properties of candidate solidified products (solidified waste and canister) as functions of composition, processing parameters, and storage conditions. The measurements are used to assure operability of the manufacturing processes and to provide data for safety analyses of high-level waste management. Our goal is to characterize the physical and chemical properties of the waste forms so thoroughly that when they are placed in retrievable storage and later in disposal, we can be confident that their behavior is known and that any changes or interactions with their environment are predictable.

THERMAL EFFECTS ON STORED GLASS - J. H. Westsik, Jr.

The purpose of this work is to determine changes in properties of high-level waste glass as functions of storage time and temperature.

72-68 Glass

Long-term leach rates for 72-68 [PW-4b-6(2.8)73-1] glass have been determined through 443 days of leaching. Figure 5 shows these leach rates in grams of glass/cm^2/d as a function of the total time leached. The three curves are based on cesium, strontium, and uranium concentration in the leachant. Devitrified samples of 72-68 glass have leach rates a factor of ten higher than the vitreous glass shown in Figure 5.

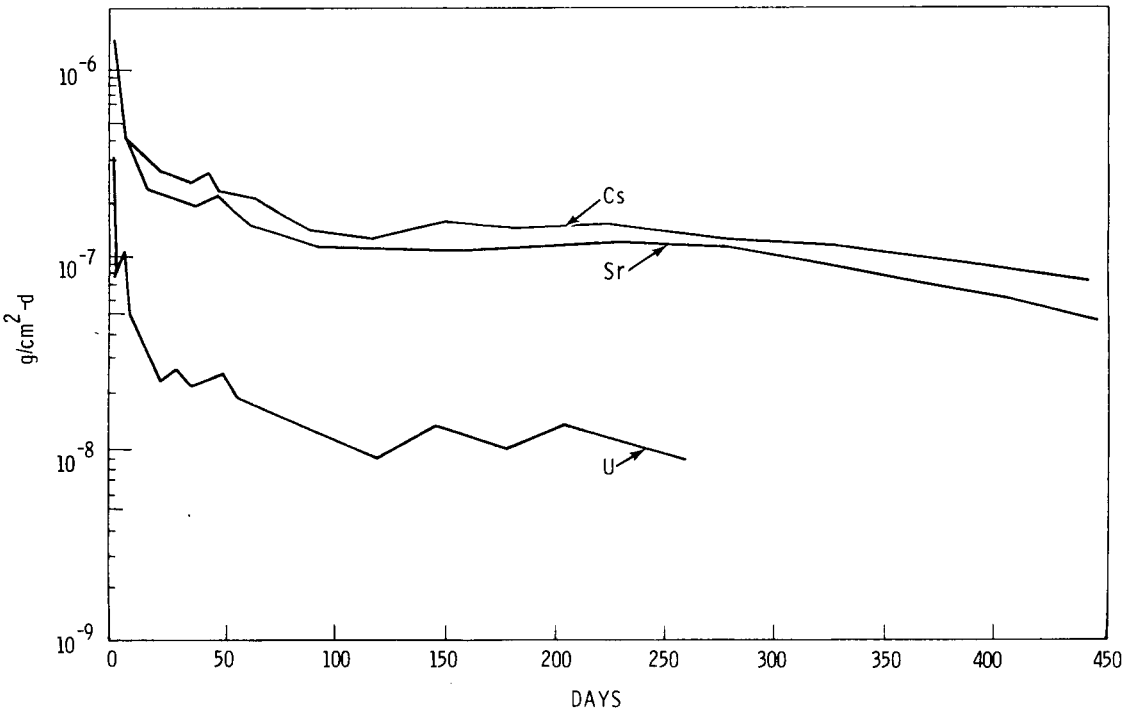

FIGURE 5. Long-Term Leach Rate of 72-68 Glass

76-68 Glass

We measured density and total open porosity for 76-68 [PW-8a-3(2:1)76-101] glass. Figure 6 shows these measurements as a function of storage temperature. Porosities are low and do not show the large variations observed for 72-68 glass.[1] Devitrification of 72-68 glass included the formation of Zn_2SiO_4, which in turn, caused microcracking in the glass. We did not find the zinc orthosilicate and resulting microcracking in 76-68 glass, and as a result the porosity remains low.

Density of 76-68 glass shows no variation with thermal treatment. The average density is 3.02 g/cc.

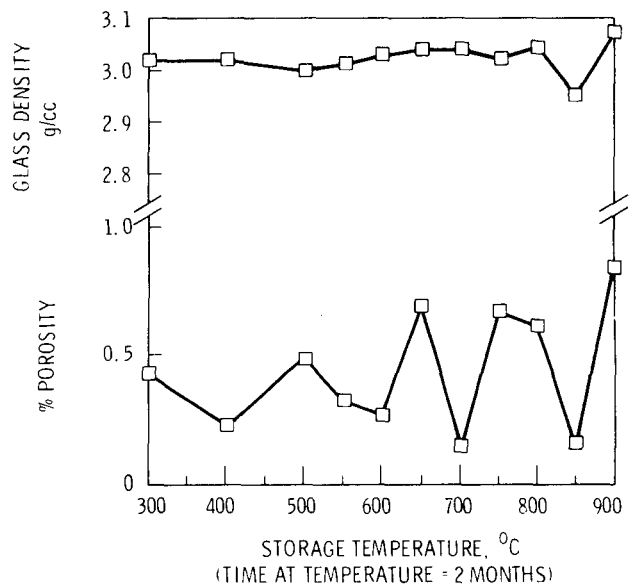

FIGURE 6. Physical Properties of 76-68 Waste Glass

ENVIRONMENTAL REACTIONS OF WASTE GLASS - J. H. Westsik, Jr.

The objective of this project is to determine the leaching behavior of waste glass in simulated storage environments.

Samples of glasses, canister materials, and geologic materials have been exposed to a salt solution similar to that which might come in contact with HLW glass in a salt formation. The exposure lasted 72 hr at 250°C and 1000 psi. Results are shown in Table 4. All samples were in a monolithic rather than a powdered configuration; thus, all surface areas were geometric calculations.

SOURCE TERM CHARACTERIZATION TASK - D. J. Bradley, R. P. Turcotte, C. E. Bigelow and J. C. Nelson
(funded by the Office of Waste Isolation)

For the first waste form studies in this task, we chose a borosilicate high-level waste glass developed to incorporate PW-8a waste composition. A resistance heated furnace produced the actinide doped glass in a glove box. For the hot cell production of the high-level waste

TABLE 4. Leach Data for Various Materials in Salt Solution

Sample	Initial Weight grams	Geometric Surface Area Cm^2	Percent Weight Loss	Grams/Cm^2 Day
Soda-Lime-Silica Glass (NBS #710)	6.1959	10.29	1.56	3.1×10^{-3}
Borosilicate Glass (NBS #717)	5.1363	10.12	.31	5.2×10^{-4}
72-68 [PW-4b-7(2.8)73-1]	6.7115	8.93	.29	7.2×10^{-4}
76-68 [PW-8a-3(2)76-101]	6.9617	9.88	.07	1.6×10^{-4}
Granite	3.0511	5.795	.36	6.4×10^{-4}
304 L Stainless Steel	9.2820	10.57	.01	4.1×10^{-5}
Inconel - 601	19.0522	12.82	.01	4.2×10^{-5}
Carbon Steel	17.5736	12.64	.02	7.4×10^{-5}

glass, we used an induction furnace for ease of operation and control. A standard bead preparation procedure for both resistance and induction melting was developed from numerous preliminary runs.

Table 5 lists the experiments outlined for characterization and leaching. The IAEA leach procedure is complemented by a static leach method to determine the effect of the buildup of corrosion products on leach rate.

Using the standard PW-8a glass made with depleted uranium, we made a resistance melter bead run. The beads will serve as archives for an NFS glass composition prior to adding actinide isotopes. They are being analyzed by metallography to determine if the bead-making process has altered the as-received standard glass. The first actinide-doped glass run was made with Cm-244; a random sample from the 250 beads is currently being analyzed by metallography.

ENGINEERING-SCALE GLASS CHARACTERIZATION - J. H. Westsik, Jr. and Y. B. Katayama

The purpose of this project is to characterize waste glasses produced on an engineering scale in the Waste Fixation Program.

Currently, we are characterizing five engineering canisters of glass in this program. Some of the processing parameters for in-can melts (ICM-16,-18,-20,-21, and -23) are shown in Table 6.

Soxhlet leach rates do not show any variation with sample position in the canister. The exception is ICM-18, where the top area showed a 2.90% weight loss compared with 0.01 to 0.37% for the glass samples taken elsewhere in the canister. The high leach area was identified as a 2 to 3 1/2 in. layer of slag on top of the otherwise homogeneous glass. Generally, the leach rates appear more dependent on the frit used rather than on any particular processing parameter.

TABLE 5. Source Term Characterization

A. Actinide Doped Glass (IAEA Leach Procedure)

	Isotopes Doped	Solutions	Replicates	Experiment
1.	$^{233}U + ^{243}Am$	5	3	15
2.	$^{239}Pu + ^{237}Np$	5	3	15
3.	^{244}Cm	3	3	9
4.	^{99}Tc	3	3	9
5.	$^{239}Pu + ^{237}Np$ Anoxic	3	3	9
6.	^{99}Tc Anoxic	3	3	9
				66

B. Actinide Doped Glasses (Static Leach Procedure)

1.	$^{239}Pu + ^{237}Np$	Salt	3*	18
2.	$^{239}Pu + ^{237}Np$	Bicarbonate	3*	18
				36

C. Full Sprectrum - Full Level Radioactive Glass

As-Formed	5	3	15
Devitrified	5	3	15
			30

*Sampled at 1 wk, 1 mo, 6 mo, 1 yr, 5 yr.

TABLE 6. Description of Canisters in Engineering Glass Characterization Program

Canister	Glass Composition	Can Size	Fins
ICM-16	PW-7a-2(1:2)75-75+1.5% Si	12" SCH 40	304L
ICM-18	PW-8a-2(1:2)75-75+1.5% Si Cs+10% RO	8" SCH 40	NONE
ICM-20	PW-7a-2(1:2)75-75+1.5% Si	8" SCH 40	E-Brite 26-1®
ICM-21	PW-7a-2(1:2.4)75-75+0.5% SiC	12" SCH 40	304L SS
ICM-23	PW-7a-2(1:2)76-199+1.5% Si	16"	304L SS

®AIRCO Vacuum Metals

Glasses made with zinc borosilicate frit 75-75 have significantly lower Soxhlet leach rates than ICM-23 glass made with borosilicate frit. Table 7 lists the leach rate ranges observed for the canisters.

The crystalline phases in ICM-16 and ICM-18 have been identified by X-ray diffraction. Tables 8 and 9 list the identified species.

TABLE 7. Soxhlet Leach Rates for ICM Glasses

	Leach Rate Range Weight Percent Loss in 72 Hours
ICM-16	0.2 - 0.5
ICM-18	0.1 - 0.4, 2.90
ICM-20	Not Determined
ICM-21	0.2 - 0.4
ICM-23	6.1 - 11.2

TABLE 8. Crystalline Phases in ICM-16 Glass

Compound	Wt%	Structure	Lattice Constants (Å)		Size (μM)
$(Ce,La)PO_4$	16	Monoclinic	a=6.77	b=7.01	30 x 20
			c=6.43	β=103°10	
$Zn_2Mo_3O_8$	3.5	Hexagonal	a=5.74	c-9.94	5 x 5
(Ce,Zr,Fe)	0.5	Cubic	a-5.36		
Ni-Te	Trace				5 diameter
$ZnCr_2O_4$	Trace				2 diameter

TABLE 9. Crystalline Phases in ICM-18 Glass

Compound	Wt%	Structure	Lattice Constants (Å)	Size (μM)
$Zn(Fe,Cr)_2O_4$	7.6	Cubic	a = 8.42	5 x 5
$(Ce,Zr,Fe)O_2$	0.2	Cubic		5 x 5
Unidentified	0.2			<5

THERMAL AND MECHANICAL SHOCK - L. R. Bunnell

The purpose of this work is to examine various factors relevant to the thermal and mechanical shock resistance of waste-containing glasses and to suggest methods for possible improvements in these properties.

One way to examine the results of in-canister melt runs is to saw and polish a full cross-section of the canister. By close observation of the specimen itself, it is possible to locate the cracks against the black glass, but it is difficult to appreciate the existing networks from a photograph. To provide a better, reproducible method for observing the cracks, we used a conventional dye penetrant.[(a)] The cracks absorb an oil-base dye by capillary action; when the excess dye is cleaned away and a fine powder is applied to the surface, the dye is absorbed by the powder. The cracks appear magnified and are seen against a white background.

(a) Spot-Check dye, cleaner, and developer, Magnaflux Corporation

Figure 7 illustrates this method with ICM-20, a canister containing PW-7a-2 calcine and 75-75 frit (1:2) with 1.5% Si additive and with fins made of E-Brite alloy. The cracks around the fins are readily visible by this technique and are caused by the higher expansion coefficient of the fins, placing the glass in compression below the temperature where it can flow. The glass probably failed in shear, judging by the crack patterns. The objective of our work is to quantify the additional surface area created by various processing changes.

In the impact testing done to date, the testing machine was limited to about 150 ft-lb. It is desirable to do some testing at higher energies, ~1500 ft-lb, to test for trends in surface area and fines production. Thus, we devised a weight with a punch-and-die assembly on the bottom, then dropped this mass on a concrete pad. At 150 ft-lb, the agreement with previous data was good; testing at 1500 ft-lb will be done shortly.

As reported in the previous quarterly, we are evaluating the strength of simulated waste-containing glasses with a diametral compression test. The scatter obtained in initial testing was judged high ($\sigma \sim 20\%$). Since the failure occurs from the flat faces of the cylinder unless it contains a large internal flaw, the ends were first chamfered; no improvement was noted. Chamfering and flame-polishing increased the average strength, but also increased the scatter. Apparently the scatter is intrinsic and will not be eliminated while still obtaining realistic results. Future testing will concentrate on close pre-testing examination and on specimens prepared in the same manner (core-drilled, with diamond sawed ends).

As part of a large characterization effort, we are making thermal expansion determinations on many specimens from recent canisters. The work is done in a push-rod dilatometer in an air atmosphere, and samples are heated at 4°C/min. Table 10 shows the glass transition temperature, dilatometric softening point, and thermal expansion coefficient for five ICM-23 specimens taken at the positions noted.

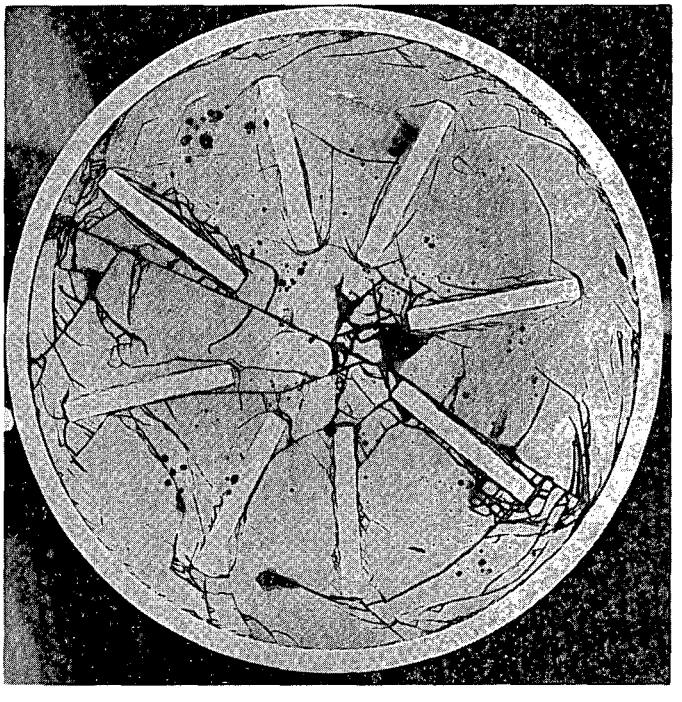

FIGURE 7. Crack Networks in ICM-20, as Revealed by Dye Penetrant Testing

TABLE 10. Thermal Expansion Parameters for ICM-23[a]

	T_G	T_S	α, $\times 10^{-6}$/°C RT-400°C
Section 1: 2-1/4 in. from bottom	525	625	9.60
Section 2: 8-1/2 in.	530	595	9.06
Section 3: 14-3/4 in.	533	575	10.0
Section 4: 21 in.	530	580	9.86
Section 5: 26-3/4 in.	525	593	9.47

(a) Total Canister Height 34.5 in.

Figure 8 is an example of the thermal expansion curves. As shown by the figure, the expansions are similar. The glass transition temperatures and thermal expansion coefficients are also similar, but the dilatometric softening point is higher at the very top, probably indicating some small composition difference in composition.

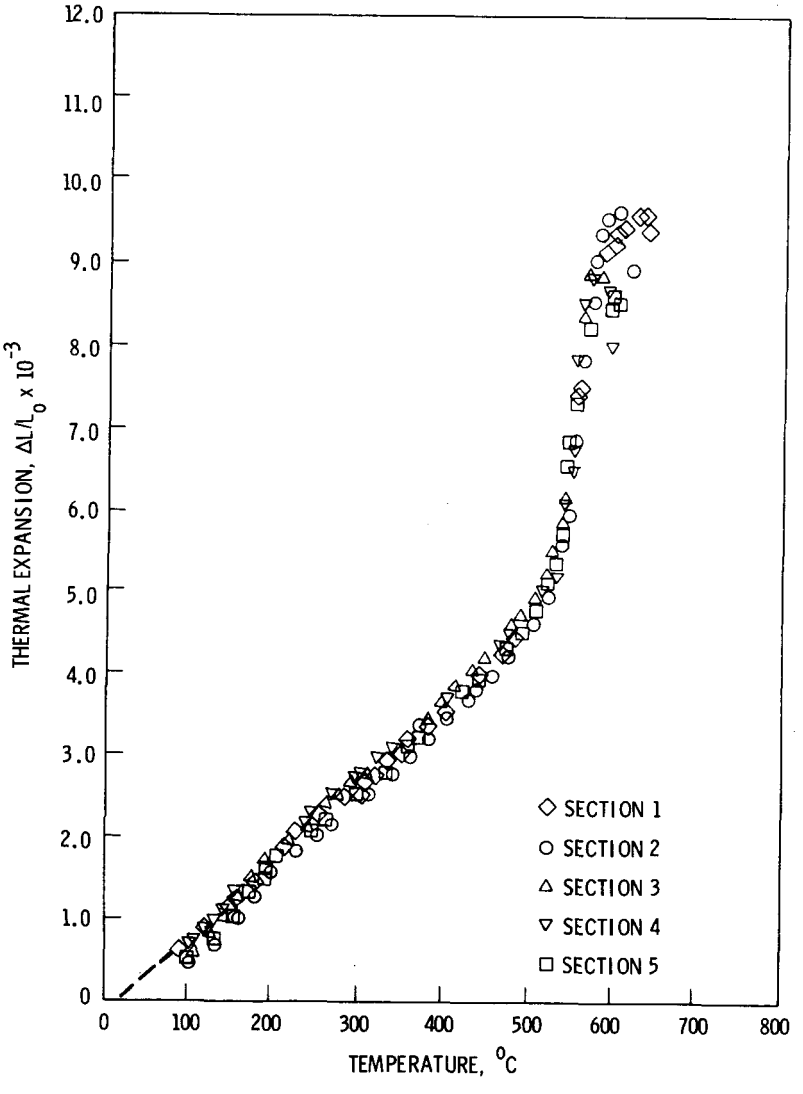

FIGURE 8. Thermal Expansion Results for ICM-23 Specimens Taken from Different Heights in the Canister

PHASE BEHAVIOR - J. W. Wald and R. P. Turcotte

This task is directed toward general understanding of the glass-making and devitrification processes. The effort is aimed primarily toward examination of phase separation by microscopy, microprobe analysis, and X-ray diffraction methods.

We have completed qualitative X-ray diffraction analysis of glass for samples held at a series of temperatures between 300°C and 900°C for one day, one week and two months. Only the fluorite phase exhibited a nucleation growth-devitrification behavior. Maximum concentrations appear to be 750°C for time periods of more than one day. The spinel phase exhibits a broad maximum at about 700°C and shows little change with anneal time.

This quarter we also developed a system to assign an "order of merit" to various glasses when they are compared to known crystalline standards. Uniform dilutions of Al_2O_3 and vitreous glass were analyzed by X-Ray diffraction and crystalline concentration. The integrated intensity for $2\theta <$ 60°C was then used to obtain a crystallinity value as Al_2O_3. Although qualitative, this provides a rapid test for glass quality, which is needed. Table 11 compares the crystallinity of several glasses.

TABLE 11. Measured Degree of Crystallinity in Waste Glasses 72-68, 76-68, and 76-183, Given in Wt%

Glass	As-Prepared	700°C-1 Week
72-68	15%	44%
76-68	4%	18%
76-183	NA	38%

A study using controlled programmed cooling from the melt temperature was conducted to cover the range of expected cooling conditions in full-sized canister melts. Using the measure of crystallinity described above, we can establish the relative sensitivity of a glass (with respect to devitrification) to cooling rate. For the reference glass 72-68, a standard cool of ∿6°C/hr gave about 40 wt% crystallinity, with 15 wt% crystallinity in the as-prepared condition. The same standard cool for NFS glass 76-68 produced about 10% crystallinity, with 4 wt% crystallinity in the as-prepared condition. From an engineering-processing standpoint, this test indicates that glass 76-68 is about four times more tolerant to slow cools from process temperatures than glass 72-68.

RADIATION EFFECTS - J. M. Rusin, and J. W. Wald

The purpose of this study is to determine the effects of radiation on the stability and physical properties of multibarrier waste forms.

The High Flux Isotope Reactor (HFIR) experiment, which neutron-irradiates pollucite to study transmutation, is continuing on schedule. The samples will be loaded the first quarter of FY-79. Hot cell facilities at ORNL will be utilized, which include shielded X-ray diffractometer, scanning electron microscope (SEM), microprobe, and metallography.

A joint program is being outlined with Dr. R. Ewing, of the University of New Mexico, to study the effect of radiation on metamictization and its implication on the crystalline components of supercalcine. Dr. Ewing will also survey the geologic history of natural minerals common to supercalcine formulations.

The qualitative X-ray diffraction results to date can be analyzed on the 3 wt% curium-doped SPC-2 supercalcine made on March 2, 1977. Table 12 compares the diffraction angles measured with no dopant and at time = 0 (with dopant); it appears that the curium may have gone into both the apatite phase and the tetragonal phase. Both of these phases shifted in diffraction angle by over 0.1°2θ, while the fluorite phase seems to have remained constant. After three months it shifted approximately 0.1°2θ. Both the fluorite phase and the tetragonal phase appear to remain at their initial (t = 0) 2θ values for up to three months.

TABLE 12. Measured Angles for Apatite, Fluorite and Tetragonal Phases Observed in 3 wt% Cm-Doped SPC-2 Supercalcine

	Apatite (213)	Fluorite (220)	Tetragonal (111)
No Dopent	48.650°2θ	48.050°2θ	29.985°2θ
t = 0	48.515	48.000	29.870
5 da	48.515	47.970	29.870
2 wk	NA	NA	NA
6 wk	48.460	48.005	29.895
3 mo	48.470	47.980	29.880

Since the fluorite phase is known to change little with radiation damage at these short times, and also since initial measurements indicated essentially no change after doping, the (220) fluorite peak will serve as an internal standard. Figure 9 shows the ratio of integrated intensities (i.e., apatite/fluorite; tetragonal/fluorite), indicating a decrease in the intensity of the apatite peak while the tetragonal peak remains basically constant.

At this point it appears as though the apatite phase may become amorphous as a result of radiation damage, while the fluorite and tetragonal phases remain unaffected. Since initial observations seemed to indicate that curium may have gone into the tetragonal phase as well, some effect may be noted in this phase too, given enough time. Further measurements should confirm or deny this possibility.

VAPORIZATION STUDIES - J. J. Gray

The purpose of this study is to investigate the vaporization behavior of fission-product-containing wastes during processing, shipment, and storage. Accident conditions involving high temperatures and breach of the container during shipment and storage are of particular interest.

We are currently investigating the possibility of reducing Cs vaporization from waste glasses by adding Al_2O_3. Figures 10 and 11 show weight loss results for 72-68 glass, whose vaporization behavior has already been reported,[2] with Al_2O_3 additions in the range of 0 to 15 wt%.

Weight loss is reduced by a factor of just over two with 10 wt% Al_2O_3, and by slightly more than that with 15 wt%. If it is assumed that the compounds $MAlSiO_4$ or $MAlSi_2O_6$ (where M represents an alkali element) are formed, then about 10.7 wt% Al_2O_3 is required to accommodate all the alkali elements in 72-68 glass.

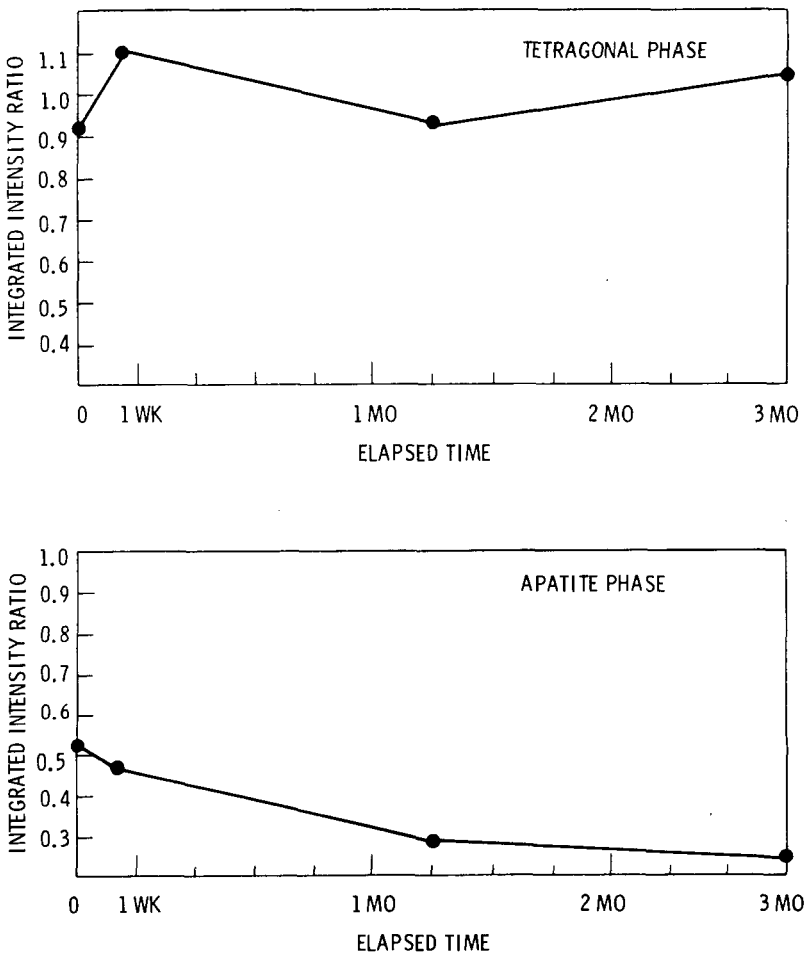

FIGURE 9. Ratio of Integrated Intensity of Apatite and Tetragonal Phases to the Fluorite Phase in 3 wt% Cm-Doped SPC-2 Supercalcine

Vapors collected from samples of 72-68 containing 10 wt% Al_2O_3 in the range of 1000 to 1200°C were chemically analyzed. Preliminary results indicate that Cs vaporization is reduced by a factor of about three by the addition of Al_2O_3. A smaller effect was observed for each of the other volatile elements: B, Na, K, Rb, Mo, Ru, and Te.

MINI-WET BASIN - Y. B. Katayama

The mini-wet basin allows the duplication of all parameters in water basin storage of canisters containing HLW product.

In the mini-wet basin of A-Cell, 324 Building, we have demonstrated canister decontamination during water basin storage. The mini-wet basin is illustrated in Figure 12.

Using two canisters filled during the Waste Solidification Engineering Prototype (WSEP) campaign, we have completed a total of three tests. Table 13 shows the WSEP data and canister storage history. The canisters were prepared for the tests by removing all loose contamination by a decontamination water spray ring.

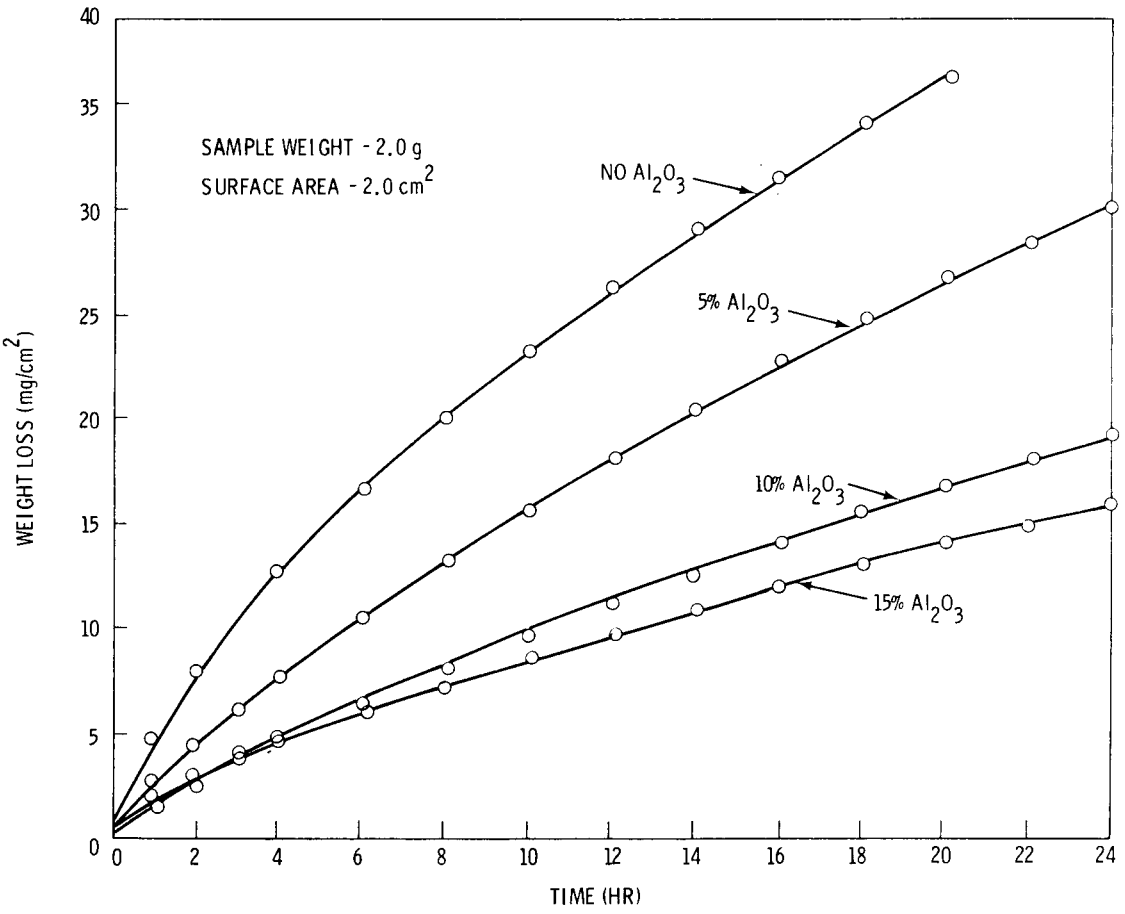

FIGURE 10. Weight Loss at 1100°C in Dry Air of 72-68 Glass Containing Various Amounts of Al_2O_3

The smearable contamination level of the canister surface was determined before and after each test by smearing a 1000 cm^2 section of the canister with a 100 cm^2 smear pad. A blank smear was used to determine the background level of A-Cell. Table 14 lists the results of the smear tests with the background levels subtracted.

Figure 13 is a graphical representation of the self-decontamination observed during the three tests. During the longest test, 86% of the initial smearable contamination was removed during storage in the mini-wet basin.

The basin water was periodically sampled and analyzed radiochemically for ^{137}Cs. Figure 14 shows the trend of ^{137}Cs concentration, d/m/ml, in the basin water during each of the three tests. In Test A, a 66-day run, the basin water line was single-valved to bypass the deionizer. The effect of contamination diffusion to the ion exchange bed is shown as a decreasing water contamination level. In Test B, a 31-day run, the basin water was valved to pass through the deionizer. In Test C, a 145-day run, the deionizer was double-valved out of the basin water recirculation system. The water recirculation was controlled at 0.5 GPM.

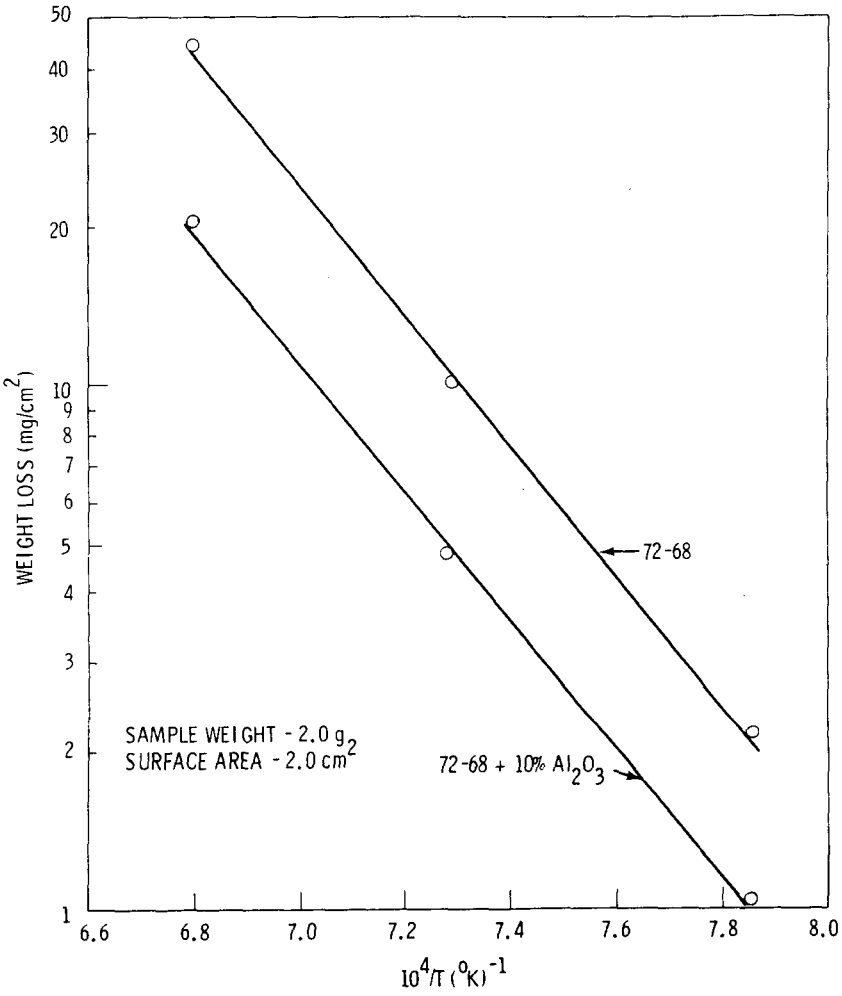

FIGURE 11. Weight Loss in Four Hours in Dry Air

No relationship between surface contamination and water contamination is apparent at this time in the testing program. The self decontamination appears to be time dependent, not dependent on the bulk concentration gradient to the basin water. The low flow rate and the resultant laminar water film on the canister wall probably precludes a valid correlation with the bulk analysis of the basin water.

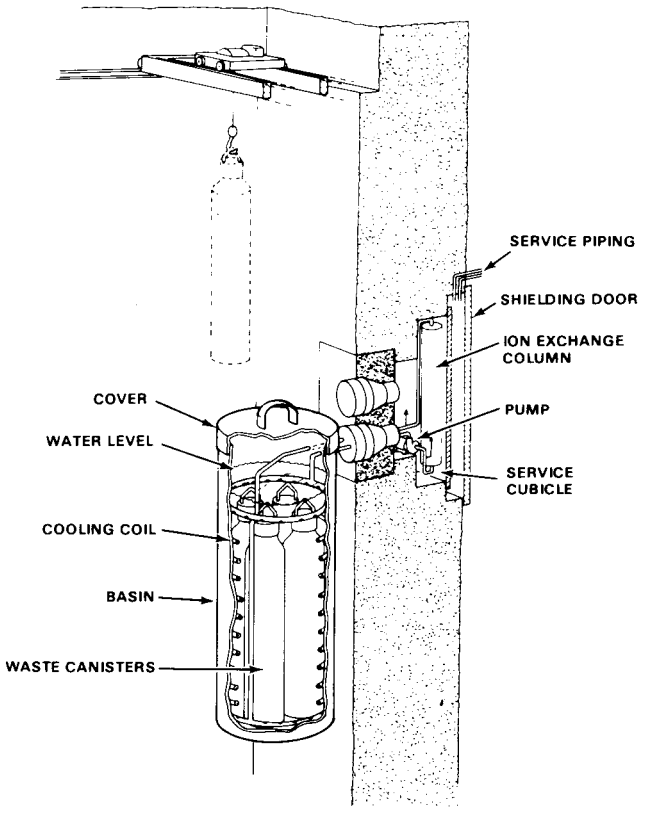

FIGURE 12. Mini-Wet Basin

TABLE 13. WSEP Canister Fill and Storage Data

Fill History	SS-7	PG-2
Fill Date	Dec. 1968	Dec. 1967
Vol. of Solids, Liters	62.0	35.0
Bulk Density, kg/liter	3.2	2.9
Fill Height, Inches	75.0	43.0
Total MCi	3.6	0.4
Total Heat Rate, kW	12.7	1.7
Heat Rate Density, W/Liter	205.0	49.0
Centerline Temp., °C	928.0	355.0
Wall Temp., °C	475.0	220.0
Radiation @ 8' in Sept. 1976, R/hr	51.0	27.0
Canister Material	304L	304L
Storage History		
Water B-Cell, Years	2-1/2	1-3/4
Air B-Cell, Years	---	---
Air A-Cell, Years	5-1/2	5-1/4
Mini Wet Basin	1/2	1/2

TABLE 14. Radiochemical Analysis Results of Smear from 1000 cm^2 of Canister Surface

Canister No. and Days	Radioisotope Measured	Initial Smear, Ci	Final Smear, Ci
SS-7, 66	^{144}Ce	2.30×10^{-7}	1.65×10^{-7}
	^{106}Ru	(a)	5.08×10^{-9}
	^{134}Cs	2.17×10^{-9}	(a)
	^{137}Cs	1.89×10^{-7}	3.72×10^{-8}
	^{125}Sb	(a)	(a)
	^{154}Eu	1.58×10^{-8}	1.46×10^{-8}
	Total	4.37×10^{-7}	2.22×10^{-7}
SS-7,31	^{144}Ce	1.65×10^{-7}	1.13×10^{-7}
	^{106}Ru	5.08×10^{-9}	5.21×10^{-9}
	^{134}Cs	(a)	(a)
	^{137}Cs	3.72×10^{-8}	2.17×10^{-8}
	^{125}Sb	(a)	1.40×10^{-9}
	^{154}Eu	1.47×10^{-8}	1.05×10^{-8}
	Total	2.22×10^{-7}	1.52×10^{-7}
PG-2, 145	^{144}Ce	7.52×10^{-7}	1.23×10^{-7}
	^{106}Ru	1.75×10^{-8}	(a)
	^{134}Cs	5.96×10^{-9}	(a)
	^{137}Cs	7.60×10^{-7}	7.11×10^{-8}
	^{125}Sb	5.41×10^{-9}	(a)
	^{154}Eu	1.25×10^{-7}	2.53×10^{-8}
	Total	1.67×10^{-6}	2.19×10^{-7}

(a) Below limits of detectability

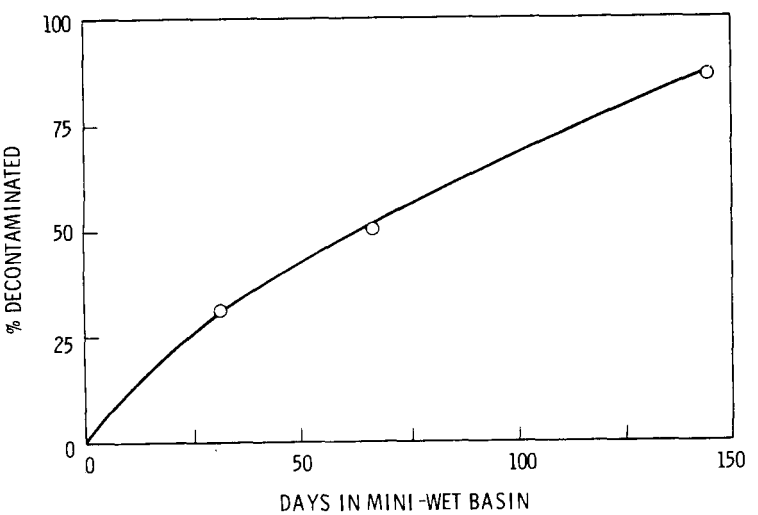

FIGURE 13. Self-Decontamination of HLW Canisters During Water Basin Storage

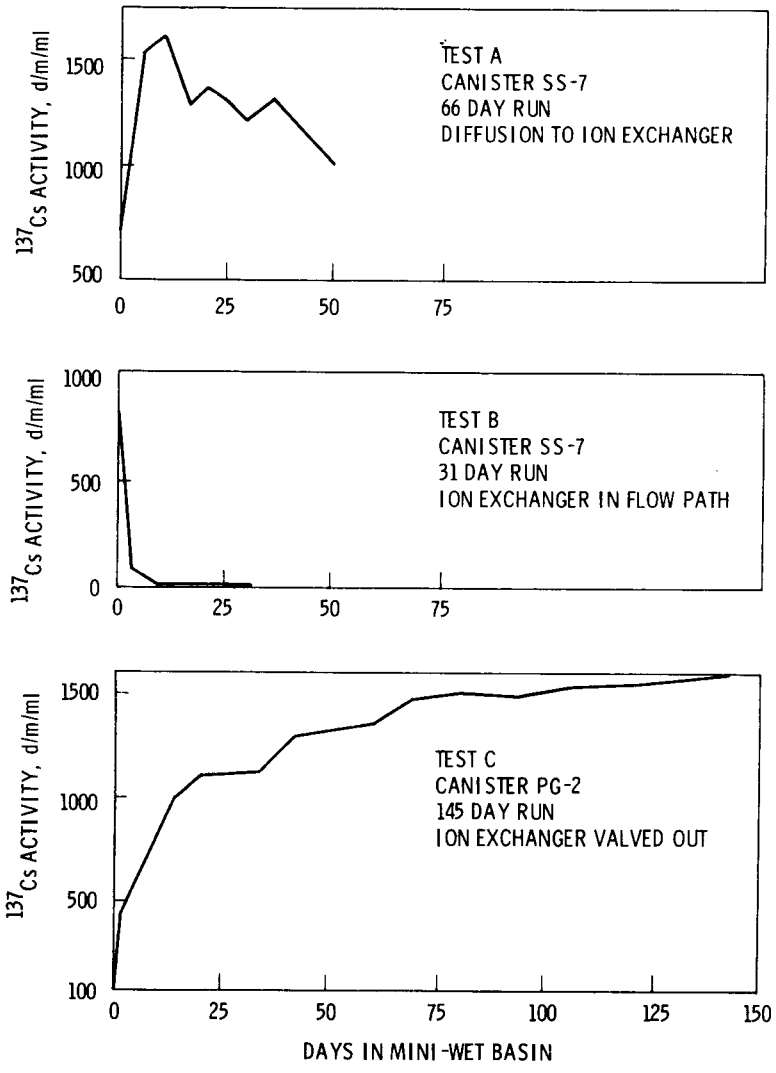

FIGURE 14. Radiochemical Analysis Results, Water Samples

SECTION 3 - ALTERNATIVE WASTE FIXATION PROGRAM

The goals of this task are to develop alternative waste fixation processes and evaluate their waste form products to assure that viable backup processes will be available if needed. The alternative processes and products are to be compared for cost and safety to silicate glass castings in large metal canisters, which are considered the current reference process and product. The alternative processes are being developed on the laboratory scale.

ENGINEERING FEASIBILITY - R. O. Lokken

The purpose of this study is to evaluate and correlate process procedures necessary to achieve the objective of the multibarrier concept.

A computer code has been developed which provides a fast and simple means of calculating mass and heat flow rates for the three multibarrier waste form processes. Three core materials are being considered: CVD-coated supercalcine, glass-coated supercalcine, and glass marbles. These three core materials are to be incorporated in one of six metal matrices:

1) cast aluminum,
2) cast aluminum-12 silicon,
3) cast lead,
4) cast lead-10 tin,
5) gravity-sintered 410 stainless steel, and
6) gravity-sintered copper.

Composite thermal conductivity of the desired waste form is calculated with the Bruggeman Variable Dispersion Equation[3] derived for spherical inclusions in a surrounding continuous phase:

$$P_2 = \frac{K_1 - K}{K_1 - K_2} \sqrt[3]{\frac{K_2}{K}}$$

where, P_2 is volume fraction of spherical inclusions

K is thermal conductivity of composite (W/cm°C)

K_1 is thermal conductivity of matrix (W/cm°C)

K_2 is thermal conductivity of spheres (W/cm°C)

The thermal conductivity of the sintered matrix materials is calculated with the porosity correction equation:[4]

$$K = K_0\left[\frac{1 - P}{1 + 10P^2}\right]$$

where, K is thermal conductivity of porous material (W/cm°C)

K_0 is thermal conductivity of dense material (W/cm°C)

P is fractional porosity

The resultant thermal conductivity values are used to calculate maximum canister diameter based on maximum allowable centerline temperatures and heat loading per canister. Maximum allowable temperatures are:

1)	CVD-coated SPC:	800°C (Cu matrix)
		1000°C (SS matrix)
2)	Glass-coated SPC:	600°C (Al-12 Si matrix)
3)	Waste-glass marbles:	300°C (Pb-10 Sn matrix)
		500°C (Al-12 Si matrix)

All temperatures are selected somewhat arbitrarily for comparative purposes. The centerline and wall temperatures are also calculated for a specific canister using the heat transfer relationships of Hoskins and Berreth.[5] The coordinate system used in the derivation is shown in Figure 15. The equations for calculating the centerline temperature, T_3, and the wall temperature, T_4, are given by:

$$(1)\quad T_4 = T_3 + \left[\frac{R_1 h_1}{k}(T_3 - T_1) + \frac{QR_1^2}{2}\right]\ln\frac{R_2}{R_1} - \frac{Q}{4k}\left(R_2^2 - R_1^2\right)$$

$$(2)\quad T_3 = \frac{k}{R_0 k h_1 + R_3 k h_2 + h_2 R_3 h_1 R_1 \ln\frac{R_2}{R_1}}\left[\frac{Q}{2}\left(R_2^2 - R_1^2\right)\left(\frac{1 + h_2 R_3}{2k}\right) + \left(\frac{R_1 R_3 h_2}{k}\ln\frac{R_2}{R_1}\right)\left(h_1 T_1 - \frac{QR_1}{2}\right) + h_1 R_0 T_1 + h_2 R_3 T_2\right]$$

where, Q is heat generation (W/m^3)

k is thermal conductivity (W/m°C)

$R_0 = R_1 - W$, W is wall thickness

$R_3 = R_2 + W$

For free convection in air with a turbulent boundary layer,

$$h_1 = 1.31\,(T_3 - T_1)^{1/3}$$

$$h_2 = 1.31\,(T_4 - T_2)^{1/3}$$

Equations 1 and 2 must be solved iteratively for T_3 and T_4 since h_1 and h_2 depend on T_3 and T_4. For waste stored in a solid cylinder, R_1 can be assumed to approach zero. Equations 1 and 2 are then reduced to:

$$(3)\quad T_4 = T_3 - \frac{QR_2^2}{4k}$$

$$(4)\quad T_3 = \frac{1}{R_3 k h_2}\left[\frac{QR_2^2}{2}\left(\frac{1 + h_2 R_3}{2k}\right) + h_2 R_3 T_2\right]$$

Equations 3 and 4 give the centerline and wall temperatures of waste stored in a solid cylinder. The output of the program is divided into four sections: 1) all input values used for a

particular process, 2) flow rates for each phase of the process, 3) annual material requirements and annual material costs, and 4) storage size requirements.

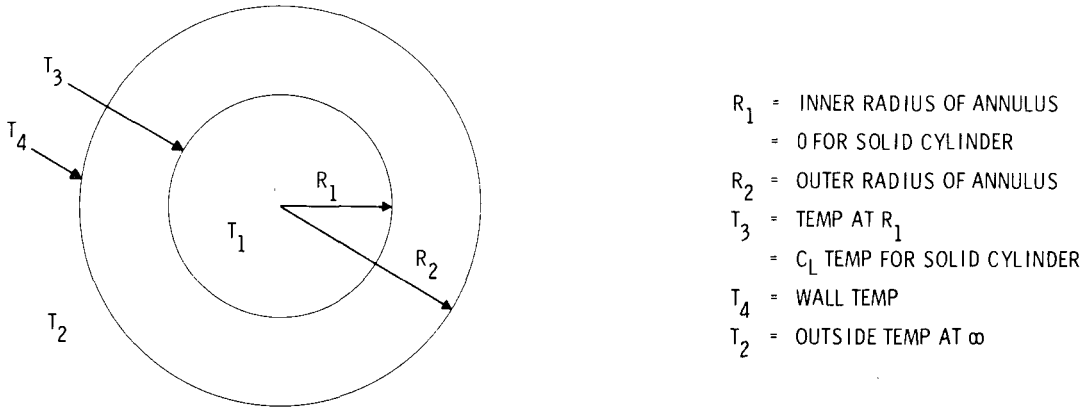

FIGURE 15. Coordinate System Used in Model for Calculating Canister Temperatures

Figure 16 shows the relationship of canister centerline temperatures to canister diameters for duplex-coated supercalcine in various matrices. The supercalcine cores have 4 mm diameters with 20 μm PyC and 60 μm Al_2O_3 coatings; sintered matrices are assumed 50% dense. Heat generation rate of supercalcine cores is 396,800 W/m^3, assuming sintered core density of 3.1 g/cc. The volume heat generation within the canister is determined by multiplying the volume fraction of supercalcine cores in the canister by their respective heat generation rate: 396,800 W/cm^3. Table 15 shows the comparative unit material costs of producing four waste forms.

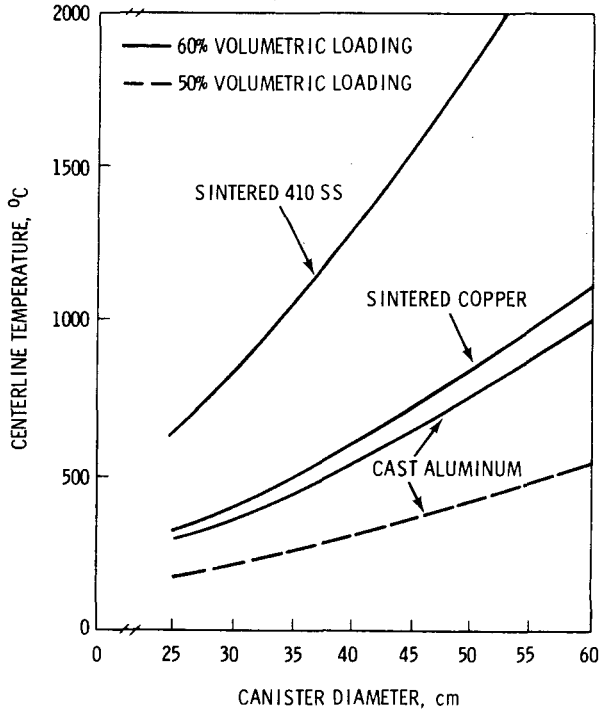

FIGURE 16. Canister Centerline Temperatures and Diameters for Duplex-Coated Supercalcine

TABLE 15. Comparison of Unit Material Costs for Multibarrier Waste Forms and Waste Glass Canisters

	Material Costs ($/kg Waste)			
	CVD Coated Supercalcine[a]	Glass Coated Supercalcine[b]	Waste Glass Marbles	Waste Glass Monolith
Additives	5.64	7.08	4.14	4.14
Matrix	2.45	5.78	1.68	--
Canisters[c]	3.21	3.59	2.66	0.90
Total	11.30	16.45	8.48	5.04

[a] Supercalcine core is 4 mm diameter, with PyC and Al_2O_3 coating thickness of 20 μm and 60 μm, respectively.

[b] Supercalcine core is 6.35 mm diameter with a frit coating thickness of 1.27 mm.

[c] Canister costs are based on canisters with a maximum allowable diameter for each specific waste form and a length of 304.8 cm. Costs were determined for each canister by using $250/m^2 of canister surface area.

GLASS MARBLE DEVELOPMENT - J. M. Rusin

The purpose of this study is to develop methods to produce waste glass marbles in remote facilities and to evaluate glass-metal matrix reactions.

Analysis of the heat treated Al-12 Si and Pb encapsulated waste glass marbles by optical microscopy has been completed. Glass-matrix reactions were not observed for the Al-12 Si sample after heat treatments of ten days at 300°C and 500°C. Reaction zones were observed in the Pb encapsulated samples; at 300°C the reaction zone appears to be in the Pb matrix, illustrated in Figure 17. The dark band between the matrix and the marble is shrinkage void that has been impregnated with the mount resin. At 500°C the Pb matrix is molten and the reaction occurs as a continuum between the Pb matrix and the glass marble, as shown in Figure 17. Further characterization will be made by SEM.

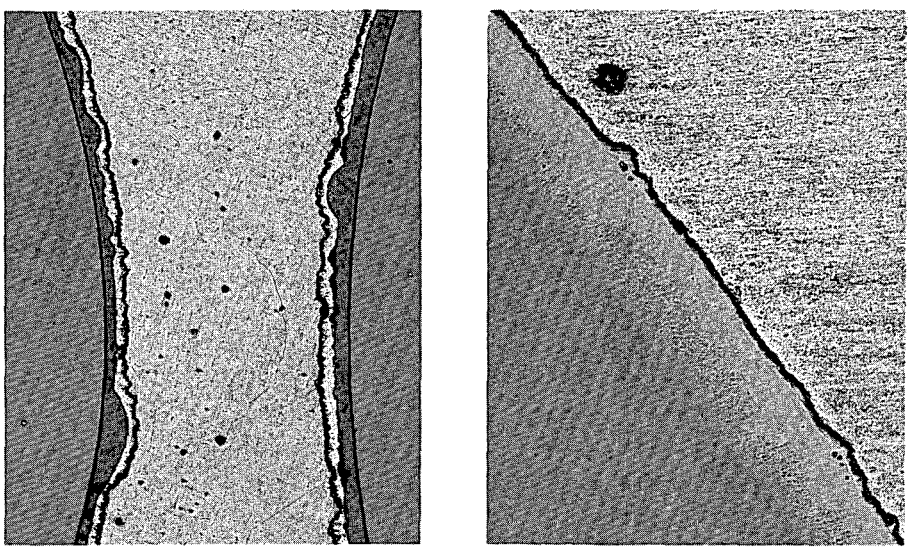

∿50X ∿250X

(a) 300°C - 10 DAYS (b) 500°C - 10 DAYS

FIGURE 17. Heat Treated Waste Glass Marbles Encapsulated in Lead

Plasma-sprayed Al coatings have been successfully applied to 3 mm and 6 mm commercial glass beads; coating thicknesses varied from 200 to 500 μm. The coatings contained some porosity. Subsequent encapsulation in Al-12 Si was successful because the coating retained its integrity, and some porosity was eliminated by penetration of the Al-12 Si alloys, shown in Figure 18. Although the purpose of this experiment was to produce samples of reduced marble loading, the successful application of metal coating to glass marbles has also been demonstrated.

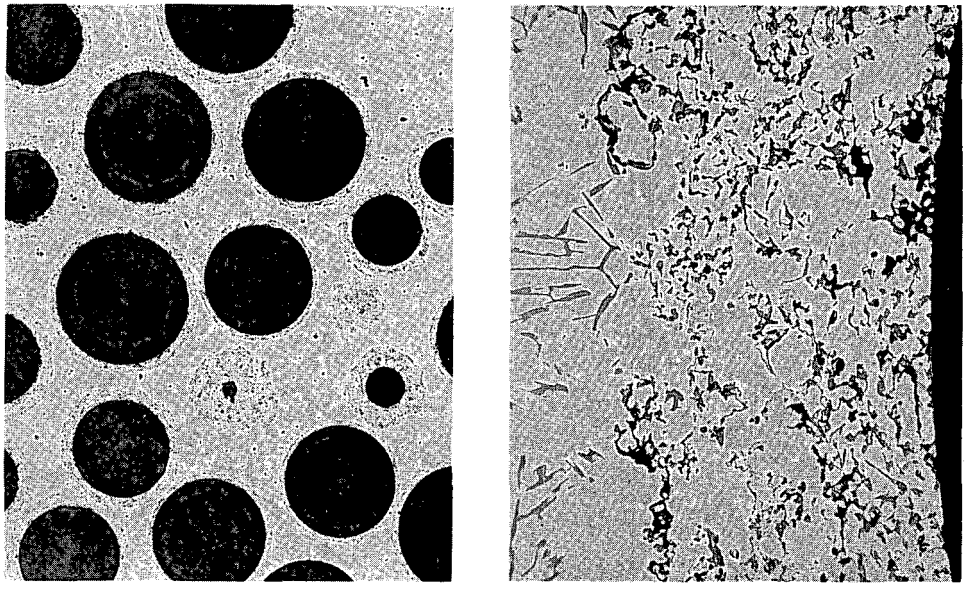

∿8X ∿200X

FIGURE 18. Aluminum Plasma Coated 3 mm Commercial Glass Beads Encapsulated in Al-12 Si

We have written a program to model the temperature distribution in the waste canister due to self-heating of spherical bodies in a matrix. The first run was made for 0.50 in. diameter waste marbles contained in a canister without any matrix. A heat generation rate of 100 watts per liter of waste glass was assumed. The results showed that the marbles in the center would begin to flow within four hours without a metal matrix.

SUPERCALCINE - G. J. McCarthy, The Pennsylvania State University

The nature of the Penn State participation in the Alternative Waste Forms Program and the supercalcine concept has been described in previous reports. Current objectives of the Supercalcine Task include: 1) refinement of existing formulations for PW-4b and PW-7 wastes, 2) development of formulations for the high Na waste PW-7a, 3) determination of crystalline phase behavior of Cs, Ru, Te, Pd, Rh and the actinides in supercalcine, and 4) consideration of the effects of radiation and transmutation on supercalcine stability.

Twenty-four high-sodium supercalcine formulations were evaluated in the last three months. Based on the results, two formulations are being given the full range of characterization. The PW-7a-based formulation of model 77-2 is:

236 RE 236 $[PO_4]$ 120 RE	$REPO_4$ $[M_{ss}]$ 15 $Ca_2RE_8[SiO_4]_6O_2$ $[A_{ss}]$	 30 Ca 90 Si
95 Mo 54 Sr + Ba	100 $(Ca,Sr,Ba)MoO_4$ $[S_{ss}]$	41 Ca
586 Na	586 $NaAlSiO_4$ [Ne]	586 Si 586 Al
64 Cs + Rb	64 $(Cs,Rb)AlSi_2O_6$	64 Al 128 Si
4 Ag + Cd	in A_{ss}	-4 Ca
100 U 106 Zr 100 Fe 12 Cr 5 Ni	as mixed oxides: F_{ss}, T_{ss}, SP_{ss}, $(Fe_2O_3)_{ss}$	
	Required Additives	67 Ca 650 Al 804 Si

Model 77-3 differs only in having the 120 extra RE, forming also as $REPO_4$, with the required addition of 120 extra $[PO_4]$ and the release of 30 Ca and 90 Si from the list of required additives by elimination of the apatite $[A_{ss}]$ phase. The scouting runs indicated that an excess of about 1.5 over the amount of (Al + Si) required for alkali (Na, Cs, Rb) fixation is necessary in each formulation to prevent significant alkali volatilization during crystallization-consolidation processing at temperatures of up to 1100°C for 2 hr. Table 16 shows the composition of 77-2 and 77-3 in weight percent of waste and additive oxides.

TABLE 16. Composition of Supercalcine 77-2 and 77-3

Oxide		Wt%	Oxide		Wt%
RE_2O_3		19.6	U_3O_8		11.0
ZrO_2		4.2	Fe_2O_3		2.6
MoO_3		4.5	Cr_2O_3		0.3
SrO		0.9	NiO		0.1
BaO		1.3		72-2	
Cs_2O		2.5	CaO		1.2
Rb_2O		0.3	Al_2O_3		16.2
CdO		0.1	SiO_2		23.7
Ag_2O		0.1		77-3	
Na_2O		5.9	CaO		0.7
P_2O_5	(77-2)	5.5	Al_2O_3		16.3
	(77-3)	8.3	SiO_2		21.2

The hot pressing method was included to give more dense and better consolidated specimens. We expected that leaching would be more sensitive to the formulation and less to its degree of

consolidation. Specimens using a 600°C denitrated batch had some "bubble-like" features, perhaps due to trapped gases arising from incomplete denitration. For this reason, a 900°C denitration was added. This pretreatment eliminated the large pore formation.

Soxhlet leach rates of the six products were tested for a total of 14 days. The values were of the same magnitude as Soxhlet leaching of PW-7a glasses (which contain about half the waste loading).

CORE AND GLASS FRIT COATING - J. M. Lukacs and C. B. Ruhter

The purpose of this task is to evaluate the disk pelletizer as a means of forming spherical pellets from calcined waste material and coating sintered pellets prior to incorporating them in a metal matrix.

Supercalcine Pellets

This quarter we prepared two new supercalcine batches in the spray calciner: SPC-3 and SPC-4. The first batch, SPC-3, is a simplified composition, while SPC-4 is the most complete simulation used to date. We studied the sintering behavior of supercalcine in detail to provide optimum sintering parameters for pelletized material. Information from vibratory compacted samples which simulated pelletized green properties is illustrated in Figure 19. Each composition has its own density vs temperature relationship; in some cases, such as in SPC-4, this may be very steep. Relatively small temperature fluctuations during processing then result in substantial density variations in the finished product.

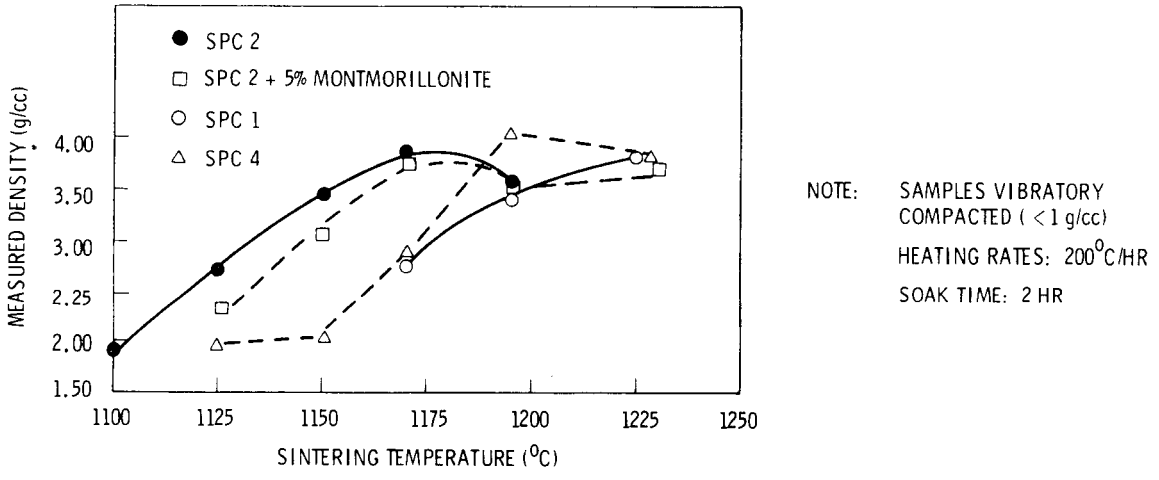

FIGURE 19. Sintered Density Vs Sintering Temperature

CHEMICAL VAPOR DEPOSITED COATINGS - M. F. Browning

The purpose of this study is to demonstrate that simulated radioactive calcined waste particles in a size range of 1 to 10 mm can be coated to protect them under environmental conditions expected during long-term storage. We have coated supercalcined particles with Al_2O_3 and/or PyC using chemical vapor deposition processes with fluidized-bed and/or mechanically-agitated particle techniques.

Our experimental effort this quarter has been directed toward:

1) application of duplex coatings by a fluidized-bed technique to 2 to 3 mm diameter supercalcined waste particles; and

2) investigation of an alternative coating-technique to the fluidized bed currently used that would be more adaptable to coating 4 to 5 mm particles.

Although the fluidized-bed technique satisfactorily applied duplex Al_2O_3/PyC coatings to smaller particles, we have experienced limited success in applying these coatings to ∿3 mm SPC-2 particles. We successfully coated ∿3 mm SPC-2 particles with PyC and extended this technique to the application of PyC to the latest batch of material received (1SPC-2), which contains particles as large as 5 mm in size. Unfortunately, the utilization of the fluidized-bed technique for applying the desired Al_2O_3 coatings to these large particles was not as satisfactory.

Continuing from last quarter, a rotating-chamber coating system replaced the fluidized-bed process used in all the previous work; 3 to 5 mm 1SPC-2 simulated waste particles were used after treatment at 1125°C for 6 hr in air. This rotating coater was used to overcoat PyC-coated pellets. The major problem in this work was the loss of the carbon coating during application of the Al_2O_3 overcoat. This was partially expected due to the oxidizing nature of the Al_2O_3-coating environment and the inability to apply Al_2O_3 coatings as rapidly in a rotating drum system as in a fluidized bed. Control over the degree of oxidation is possible by adjusting the reactant concentration since one of the reactants is hydrogen. Unfortunately, as the degree of oxidation is reduced, the coating rate is also decreased drastically.

Several attempts to circumvent the oxidation of the PyC coating when applying Al_2O_3 coatings were made with essentially no success. Therefore, the use of SiO_2 in place of Al_2O_3 was investigated because of the increased potential of satisfactorily applying it in a drum coater over a PyC coating. Alumina was initially selected as the most desirable oxide coating because of its leach resistance. However, since the outer coating's main function is now oxidation protection, SiO_2 should be a suitable replacement.

We developed a system for overcoating with SiO_2 supercalcined particles (1SPC-2, 3- and 5-mm) which had been heat-treated for 6 hr at 1125°C in air and coated with ∿40 μm of PyC in a fluidized-bed system without loss of the PyC layer. This was done in the rotating drum system using the orthosilicate procedure. Operation of the system was relatively trouble-free and the coatings appeared to be dense and uniform in thickness. However, the SiO_2 coating of several of the particles was observed to be cracked.

METAL MATRIX - K. R. Sump

The purpose of this study is to develop a metal matrix for increasing the thermal conductivity and impact strength of containers for high-level waste.

This quarter we used two new materials for matrix evaluation: 1) aluminum-318 magnesium, vacuum-cast pure and with 3 mm and 6 mm glass spheres, and 2) aluminum bronze, successfully gravity-sintered at 950°C for 8 hr in a dynamic vacuum. A higher sintering temperature is

required for the aluminum bronze than for the pure copper. Additional samples with various matrices were cast for characterization studies. The metal matrix fabrications are summarized in Table 17.

TABLE 17. Metal Matrix Fabrications at PNL

Metal Matrix	Method of Fabrication	Waste Form Dispersed in Metal Matrix
Lead	Cast	None, glass marbles, simulated waste glass marbles
Pb-5 Sn	Cast	None, glass marbles, simulated waste glass marbles
Pb-10 Sn	Cast	None, glass marbles, simulated waste glass marbles, uncoated supercalcine
Pb-6 Sb	Cast	None, glass marbles
Aluminum	Cast	None, glass marbles
Al-12 Si	Cast	None, glass marbles, simulated waste glass marbles, uncoated supercalcine, Al clad glass marbles
Al-3,8 Mg	Cast	None, glass marbles
Copper	Gravity Sintered	None, Al_2O_3 spheres uncoated supercalcine
Manganese Bronze	Cast	None, Al_2O_3 grinding balls
Aluminum Bronze	Gravity Sintered	None
Miscellaneous Brasses	Gravity Sintered	None, uncoated calcine
Stainless Steel 316, 410, and/or 304	Gravity Sintered	None, Al_2O_3 sphere, uncoated supercalcine, Al_2O_3 coated supercalcine PyC/Al_2O_3 coated supercalcine
Iron and Alloy Steels	Gravity Sintered	None

Pure supercalcine (SPC-2) samples were fabricated with cast or gravity-sintered matrices of Al-12 Si, Pb-10 Si, 316 SS and pure copper. Considerable discoloration of the stainless steel matrix occurred during the gravity-sintering process. The other samples had a good appearance.

CHARACTERIZATION - J. M. Rusin

The purpose of this study is to determine the physical, mechanical, and chemical properties of multibarrier waste forms for optimization of this product type.

Screening of impacted gravity-sintered matrix samples has been completed. Supercalcine was separated from the 410 stainless steel with an electromagnet. Particle size distribution for the supercalcine and metal matrix is plotted on Figure 20 for several impact forces. The percent finer than 37 μm does not exceed 2%. The effect of supercalcine loading is shown in Figure 21. Two samples, one at 40% and the other at 60% loading, were impacted at 158.4 ft-lb.

The reduction in loading greatly reduced the fine particulate formation. The fines distribution for supercalcine is compared to that for an ICM-11 sample in Figure 22. The waste loading should be taken into account to provide a meaningful comparison. The fine particulate from the supercalcine would contain 2.4 times the waste content of a typical waste glass.

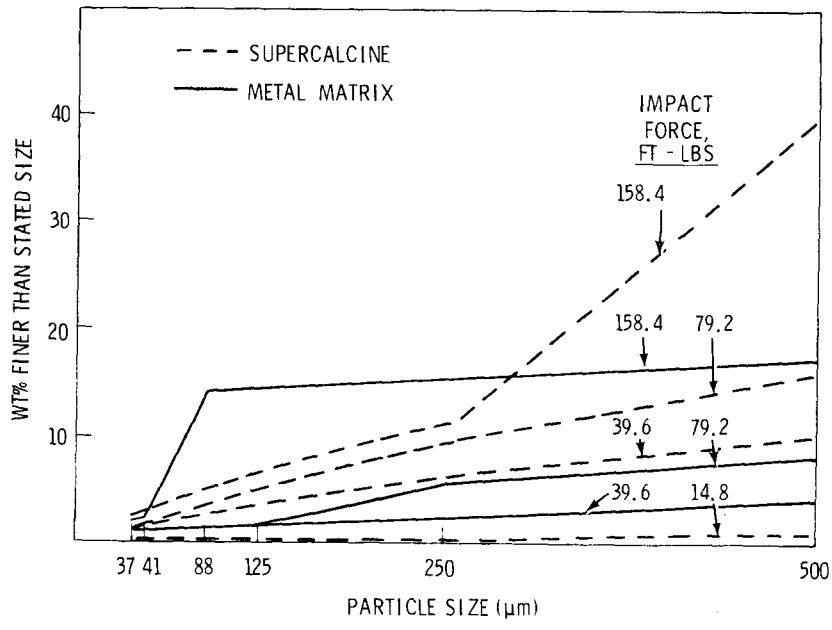

FIGURE 20. Particle Size Distribution for Impacted Al_2O_3 Coated Supercalcine in 410 Stainless Steel Matrix

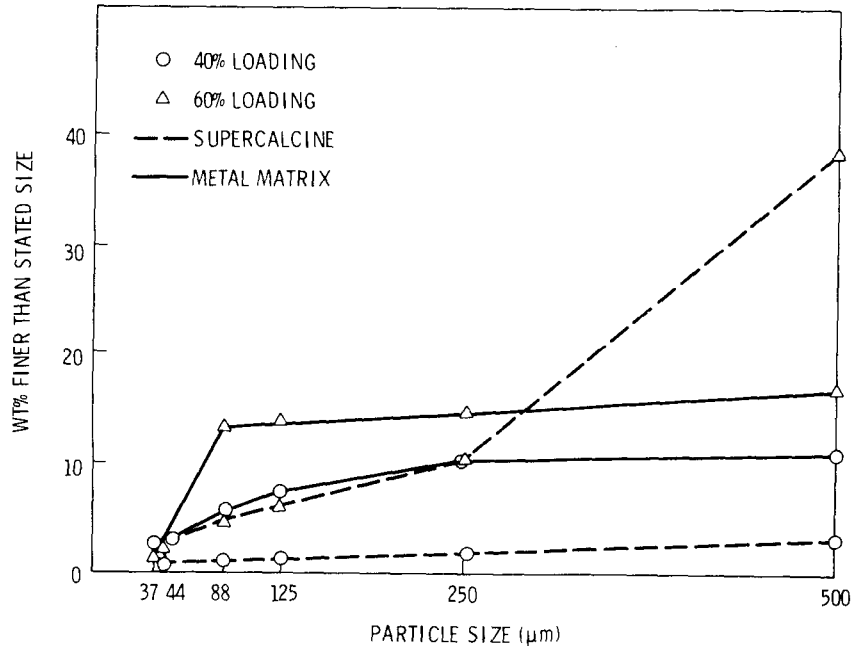

FIGURE 21. Effect of Supercalcine Loading Upon Particle Size Distribution after Impact at 158.4 ft-lb

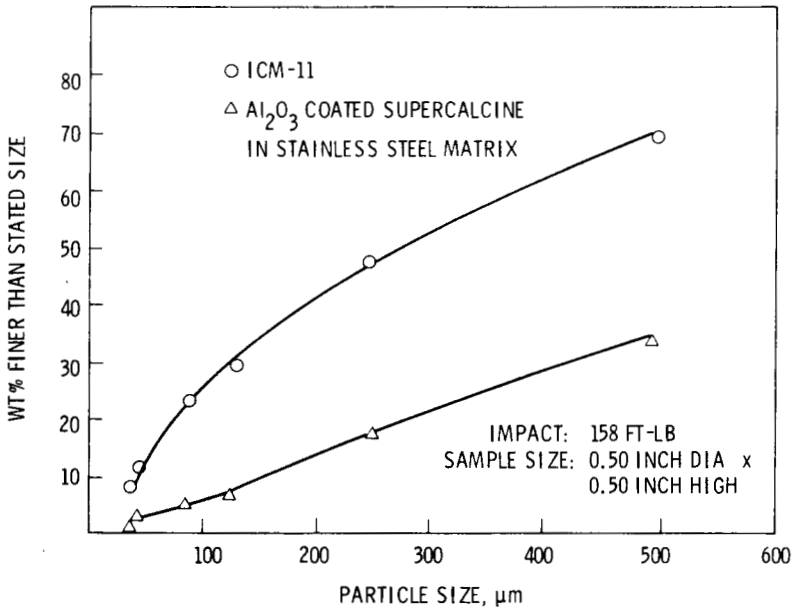

FIGURE 22. Particle Size Distribution of Impacted ICM-11 and Supercalcine Samples

Gravity-sintered Cu samples, 0.50 in. in diameter by 0.50 in. high, have been impacted to compare them to previously impacted 410 stainless steel Al-12 Si and Pb matrix samples. Figure 23 compares the compilation for all four samples to the impact force. The gravity-sintered Cu does not offer as much impact resistance as gravity-sintered 410 stainless steel.

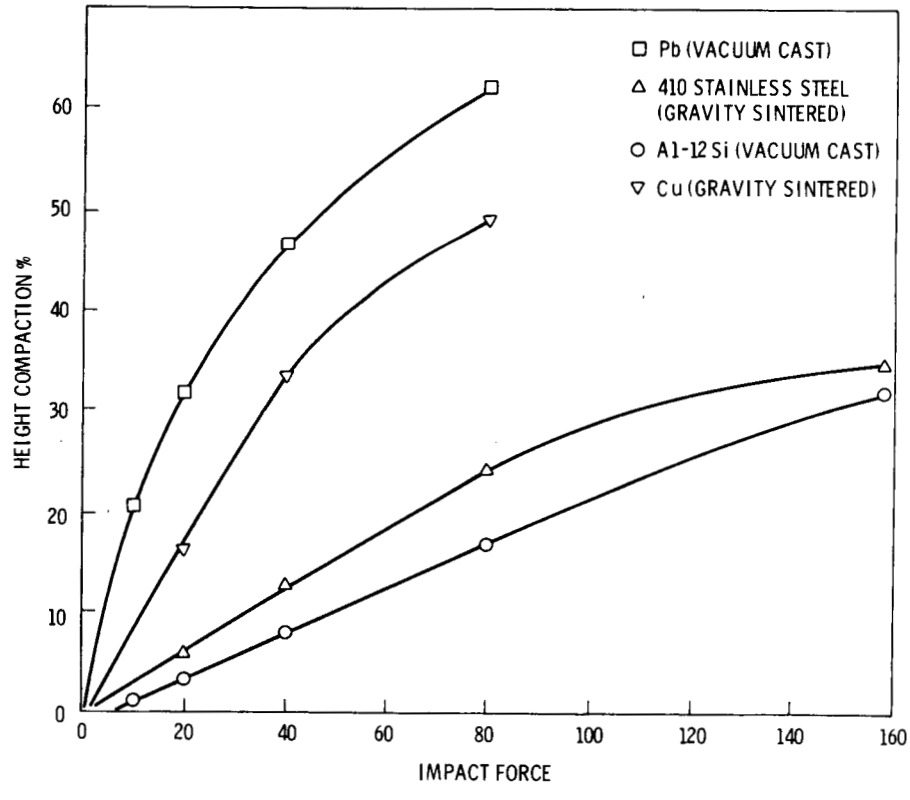

FIGURE 23. Compaction of 0.50 in. Diameter Matrix Samples by Impact

We produced samples of uncoated supercalcine (SPC-2) cores encapsulated in vacuum-cast Pb and Al-12 for characterization. The results from metallography show no evidence of reaction between the supercalcine and vacuum cast Pb or Al-12 Si. Polished sections are illustrated in Figure 24. Presently, we are characterizing samples of uncoated supercalcine encapsulated in gravity-sintered Cu and 316 stainless steel.

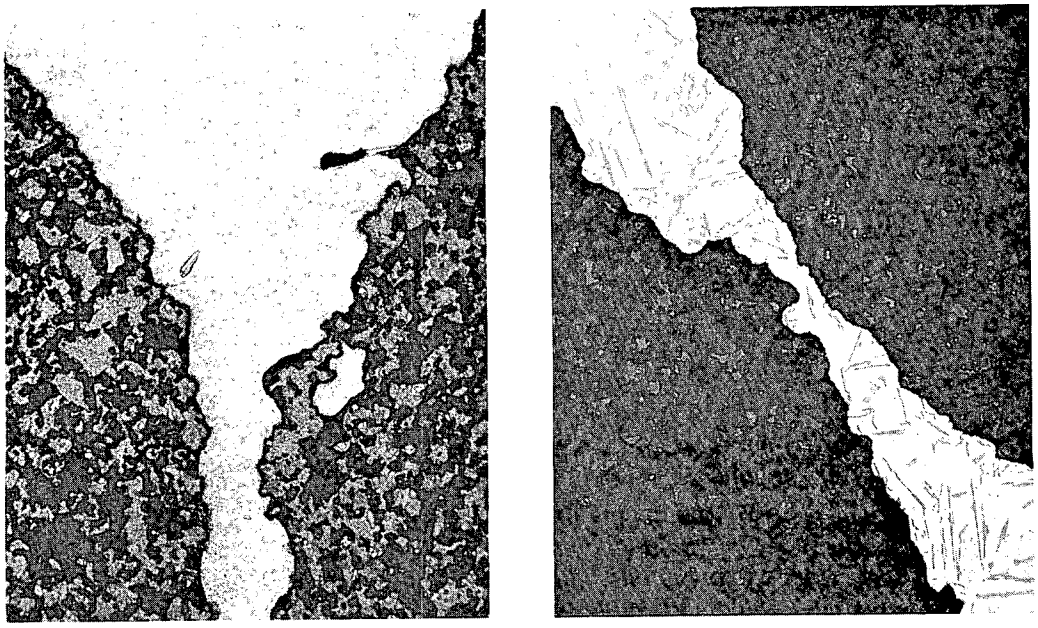

∿200X ∿200X

(a) Pb-10 Sn (b) Al-12 Si

FIGURE 24. Uncoated Supercalcine (SPC-2) Encapsulated in Vacuum Cast Pb-10 Sn and Al-12 Si

REFERENCES

1. J. H. Westsik, Jr. "Thermal Effects on Stored Glass," Quarterly Progress Report, Research and Development Activities, Waste Fixation Program, BNWL-2070, Battelle, Pacific Northwest Laboratories, Richland, Washington, 1976.

2. W. J. Gray, Volatility of a Zinc Borosilicate Glass Containing Simulated High-Level Radioactive Waste, BNWL-2111, Battelle, Pacific Northwest Laboratories, Richland, WA 99352, October 1976.

3. D. A. G. Bruggeman, "Dielectric Constant and Conductivity of Mixtures of Isotropic Materials," Annalen Physik, 24: 636, 1935.

4. J. C. Y. Koh and A. Fortini, Thermal Conductivity and Electrical Resistivity of Porous Material, NASA Cr-12-854, 1971.

5. A. P. Hoskins and J. R. Berreth, Heat Transfer Considerations in the Canister Storage of High-Level Solidified Wastes, ICP-1090, 1976.

DISTRIBUTION

No. of Copies

UNITED STATES

A. A Churm
DOE Chicago Patent Group
9800 South Cass Avenue
Argonne, IL 60439

Deputy Director for Fuels and Materials
NRC Directorate of Licensing for Fuels and Materials
Silver Springs, MD 20910

W. P. Bishop
Assistant Director for Radioactive Waste Management Branch
NRC Division of Materials and Fuel Cycle Facility Licensing
Washington, DC 2054

W. G. Belter
DOE Division of Biomedical and Environmental Research
Earth Sciences Branch
Washington, DC 20545

W. A. Brobst
DOE Division of Environmental Control Technology
Washington, DC 20545

W. E. Mott
DOE Division of Environmental Control Technology
Washington, DC 20545

G. W. Cunningham
DOE, Administrator for Nuclear Energy Programs
Washington, DC 20545

R. B. Chitwood
DOE Division of Nuclear Power Development
Washington, DC 20545

T. C. Chee
DOE Division of Waste Management
Washington, DC 20545

C. R. Cooley
DOE Division of Waste Management
Washington, DC 20545

R. L. Morgan
DOE Division of Waste Management
Washington, DC 20545

No. of Copies

R. G. Romatowski
DOE Division of Waste Management
Washington, DC 20545

C. W. Kuhlman
DOE Division of Waste Management
Washington, DC 20545

C. H. George
DOE Division of Waste Management
Washington, DC 20545

C. A. Heath
DOE Division of Waste Management
Washington, DC 20545

G. Oertel
DOE Division of Waste Management
Washinton, DC 20545

A. F. Perge
DOE Division of Waste Management
Washington, DC 20545

D. L. Vieth
DOE Division of Waste Management
Washington, DC 20545

R. D. Walton
DOE Division of Waste Management
Washington, DC 20545

DOE Idaho Operations Office
P.O. Box 2108
Idaho Falls, ID 83401

J. B. Whitsett
DOE Idaho Operations Office
P.O. Box 2108
Idaho FAlls, ID 83401

J. J. Schreiber
DOE Oak Ridge Operations Office
P.O. Box X
Oak Ridge, TN 37830

John Van Cleve
DOE Oak Ridge Operations Office
P.O. Box X
Oak Ridge, TN 37830

No. of
Copies

E. S. Goldberg
DOE Savannah River Operations
Office
P.O. Box A
Aiken, SC 29801

267 DOE Technical Information
Center

A. P. Roeh, Manager
Allied Chemical Corporation
550 2nd Street
Idaho Falls, ID 83401

J. R. Berreth
Allied Chemical Corporation
550 2nd Street
Idaho Falls, ID 83401

R. A. Brown
Allied Chemical Corporation
550 2nd Street
Idaho Falls, ID 83401

C. A. Hawley
Allied Chemical Corporation
550 - 2nd Street
Idaho Falls, ID 83401

D. A. Knecht
Allied Chemical Corporation
550 - 2nd Street
Idaho Falls, ID 83401

Allied Chemical Corporation
(File Copy)
550 - 2nd Street
Idaho Falls, ID 83401

R. A. Buckham
Allied-General Nuclear Service
P. O. Box 847
Barnwell, SC 29812

A. Williams
Allied General Nuclear Service
P. O. Box 847
Barnwell, SC 29812

J. L. Jardine
Argonne National Laboratory
9700 South Cass Avenue
Argonne, IL 60439

M. M. Steindler/ L. E. Trevorrow
Argonne National Laboratory
9700 South Cass Avenue
Argonne, IL 60439

No. of
Copies

J. M. Batch
Battelle Memorial Institute
505 King Ave.
Columbus, OH 43201

Wayne Carbiener
Battelle Memorial Institute
505 King Ave.
Columbus, OH 43201

J. D. Duguid
Battelle Memorial Institute
505 King Ave.
Columbus, OH 43201

R. E. Heineman
Battelle Memorial Institue
505 King Ave.
Columbus, OH 43201

J. Kircher
Battelle Memorial Institute
505 King Ave.
Columbus, OH 43201

Don Moak
Battelle Memorial Institute
505 King Ave.
Columbus, OH 43201

Ken Yates
Battelle Memorial Institute
Rm 13 - 3091
505 King Ave.
Columbus, OH 43201

Brookhaven National Laboratory
Reference Section
Information Division
Upton, Long Island, NY 11973

M. Steinberg
Brookhaven National Laboratory
Upton, Long Island, NY 11973

Combustion Divison
Combustion Engineering, Inc.
Windsor, CT 06095

B. Adams
Corning Glass Works
Technical Staffs Division
Corning, NY 14830

E. Vejvoda, Director
Chemical Operations
Rockwell International
Rocky Flats Plant
P.O. Box 464
Golden, CO 80401

No. of Copies

M. D. Boersma
duPont Company, Aiken (DOE)
E. I. duPont DeNemours and Company
Savannah River Laboratory
Aiken, SC 29801

C. H. Ice
E. I. duPont DeNemours and Company
Savannah River Laboratory
Aiken, SC 29801

A. S. Jennings
E. I. duPont DeNemours and Company
Savannah River Laboratory
Aiken, SC 29801

Leon Meyers
E. I. duPont DeNemours and Company
Savannah River Laboratory
Aiken, SC 29801

P. H. Permar
duPont Company, Aiken (DOE)
E. I. duPont DeNemours and Company
Savannah River Laboratory
Aiken, SC 29801

H. Henning
Electric Power Research Institute
3412 Hillview Avenue
P.O. Box 10412
Palo Alto, CA 94301

Environmental Protection Agency
Technology Assessment Division (AW-559)
Office of Radiation Programs
Washington, DC 20460

R. G. Barnes
General Electric Company
175 Curtner Avenue (M/C 160)
San Jose, CA 95125

L. H. Brooks
Gulf Energy and Environmental Systems
P. O. Box 81608
San Diego, CA 92138

2 Central Research Library
Document Reference Section
Oak Ridge National Laboratory (DOE)
Oak Ridge, TN 37830

3 Los Alamos Scientific Laboratory (DOE)
P.O. Box 1663
Los Alamos, NM 87544

No. of Copies

C. J. Kershner
Monsanto Research Corporation
Mound Laboratory
P.O. Box 32
Miamisburg, OH 45342

John Pomeroy
Technical Secretary
National Academy of Sciences
Committee of Radioactive Waste Management
National Research Council
2101 Constitution Avenue
Washington, DC 20418

2 J. P. Duckworth
Plant Manager
Nuclear Fuel Services, Inc.
P.O. Box 124
West Valley, NY 14171

J. G. Cline, General Manager
NYS Atomic Space and Development Authority
230 Park Avenue, RM 2425
New York, NY 10017

Oak Ridge National Laboratory (DOE)
Central Research Library
Document Reference Section
P.O. Box X
Oak Ridge, TN 37830

E. H. Kobish
Solid State Division
Oak Ridge National Laboratory
Oak Ridge, TN 37830

G. J. McGarthy
Pennsylvania State University
Materials Research Laboratory
University Park, PA 16802

D. R. Anderson
Sandia Laboratories
Albuquerque, NM 87107

J. K. Johnstone
Sandia Laboratories
Albuquerque, NM 87107

W. Weart
Sandia Laboratories
Albuquerque, NM 87107

J. Sivinshi
Sandia Laboratories
Albuquerque, NM 87107

No. of Copies

J. O. Blomeke
Union Carbide Corporation (ORNL)
Chemical Technology Division
P.O. Box Y
Oak Ridge, TN 37830

2 D. E. Ferguson
Union Carbide Corporation (ORNL)
Chemical Technology Division
P.O. Box Y
Oak Ridge, TN 37830

H. W. Godbee
Union Carbide Corporation (ORNL)
Chemical Technology Division
P. O. Box Y
Oak Ridge, TN 37830

W. C. McClain
Union Carbide Corporation (ORNL)
Chemical Technology Division
P.O. Box Y
Oak Ridge, TN 37830

R. A. Beall
U. S. Department of Interior
Bureau of Mines
Albany Research Center
1450 W. Queen Avenue
Albany, OR 97321

R. G. Post
College of Engineering
University of Arizona
Tucson, AZ 85721

S. E. Logan
University of New Mexico
Albuquerque, NM 87131

FOREIGN

2 International Atomic Energy
..Agency
Kartner Ring 11
P.O. Box 590
A-1011, Vienna, AUSTRIA

Rene Amavis
EURATOM
Health Physics Division
29, Rue Aldringer
Luxembourg, BELGIUM

G. G. Strathdee
Atomic Energy of Canada, Ltd.
W.N.R.E. Pinawa, Manitoba
ROE 1LO
CANADA

No. of Copies

M. Tomlinson
Director of Chemistry and
Materials Science Division
Atomic Energy of Canada Ltd.
Whiteshell Nuclear Research
Establishment
Pinawa, Manitoba, CANADA

K. D. B. Johnson
Atomic Energy Research
Establishment,
Harwell, Didcot,
Berks, ENGLAND

J. A. C. Marples
Atomic Energy Research
Establishment
Harwell, Didcot,
Berks, ENGLAND

D. W. Clelland
United Kingdom Atomic Energy
Authority
Risley, ENGLAND

P. J. Regnaut
Centre d'Etudes Nucleaires
de Fontenay-aux Roses
Boite Postale 6
92 - Fontenay-aux-Roses
FRANCE

Y. J. Sousselier
Center d'Etudes Nucleaires
de Fontenay-aux Roses
Boite Postale 6
92 - Fontenay-aux Roses
FRANCE

Bundesministerium für Forschung
und Technologie
Stressemannstrasse 2
5300 Bonn
GERMANY

Center for Atomic Energy
Documentation (ZAED)
Attn: Dr. Mrs. Bell
P.O. Box 3640
7500 Karlsruhe
GERMANY

Hans W. Levi
Hahn-Meitner Institut
1 Berlin 39
Glienickerstr. 100
GERMANY

No. of
Copies

H. Krause
Kernforschungszentrum Karlsruhe
GmbH (KfK)
Postfach 3640
D7500 Karlsruhe
GERMANY

R. V. Amalraj
C.W.M.F. Project
P.O. Kalpakkam
Chingleput Dist.
Tamil Nadu, INDIA

N. S. Sunder Rajan
Bhabha Atomic Research Centre
Government of India
Hall No. 5
Trombay
Bombay 8S
INDIA

Dr. Piero Risolute,
Head, Radioactive Waste Program
Plant Engineering Dept.
Agip Nucleare
Milano
C. so di Porta Romana, 68
ITALY

F. Gera
CHEN
CSN Casaccia L.I.S.
C.P. 2400, 00100
Rome
ITALY

S. Tashiro
Japan Atomic Energy
Research Institute
Environmental Safety
Research Laboratory
1-1-13, Shibashi
Minatopku, Tokyo
JAPAN

ONSITE

5 DOE Richland Operations Office

R. B. Goranson
B. D. Guilbeault
M. J. Shupe
D. J. Squires
M. J. Zamorski

11 Rockwell Hanford Operations

H. Babad
R. A. Deju
R. J. Gimera

No. of
Copies

J. D. Kaser
E. J. Kosiancic
M. J. Kupfer
C. M. Manry
J. H. Roecker
W. W. Schultz
D. D. Wodrich
File Copy

3 Exxon Nuclear Company

S. J. Beard

1 Joint Center for Graduate Study

J. Cooper

2 United Nuclear Industries, Inc.

T. E. Dabrowski
A. E. Engler

1 Westinghouse Hanford Company

A. G. Blasewitz

117 Battelle-Northwest

T. W. Ambrose
W. J. Bjorklund
H. T. Blair
W. F. Bonner
D. J. Bradley
J. L. Buelt
R. L. Bunnell
H. C. Burkholder
N. E. Carter
C. C. Chapman
L. A. Chick
T. D. Chikalla
M. O. Cloninger
J. W. Finnigan
A. A. Garrett
W. J. Gray
M. S. Hanson
J. C. Hartl
O. F. Hill
J. H. Jarrett
Y. B. Katayama
W. S. Kelly
R. S. Kemper
D. E. Knowlton
D. K. Kreid
D. E. Larson
J. M. Lukacs
R. P. Marshall
J. L. McElroy (10)
J. S. McPherson (3)
G. B. Mellinger
J. E. Mendel (25)
R. E. Nightingale

No. of
Copies

D. E. Olesen
C. R. Palmer
A. M. Platt
D. L. Prezbindowski (2)
F. P. Roberts
W. A. Ross (25)
J. M. Rusin
D. H. Siemens
S. C. Slate
R. T. Treat
R. P. Turcotte
H. H. Van Tuyl
J. W. Wald
W. E. Weber
J. H. Westsik, Jr.
L. D. Williams
W. K. Winegardner
Technical Information (5)
Publishing Coordination (2)